

## Bystander responses impact accurate detection of murine and human antigen-specific CD8 T cells

Matthew D. Martin, ... , Robert A. Seder, Vladimir P. Badovinac

*J Clin Invest.* 2019. <https://doi.org/10.1172/JCI124443>.

Research In-Press Preview Immunology

Induction of memory CD8 T cells is important for controlling infections such as malaria HIV/AIDS, and for cancer immunotherapy. Accurate assessment of antigen (Ag)-specific CD8 T-cells is critical for vaccine optimization and defining correlates of protection. However, conditions for determining Ag-specific CD8 T-cell responses ex-vivo using ICS may be variable, especially in humans with complex antigens. Here, we used an attenuated whole parasite malaria vaccine model in humans and various experimental infections in mice to show that the duration of antigenic stimulation and timing of brefeldin A (BFA) addition influences the magnitude of Ag-specific and bystander T cell responses. Indeed, following immunization with an attenuated whole sporozoite malaria vaccine in humans, significantly higher numbers of IFN- $\gamma$  producing memory CD8 T-cells comprised of antigen specific and bystander responses were detected by increasing the duration of Ag-stimulation prior to addition of BFA. Mechanistic analyses of virus-specific CD8 T-cells in mice revealed that the increase in IFN $\gamma$  producing CD8 T-cells was due to bystander activation of Ag-experienced memory CD8 T-cells, and correlated with the proportion of Ag-experienced CD8 T-cells in the stimulated populations. Incubation with anti-cytokine antibodies (ex. IL-12) improved accuracy in detecting *bona-fide* memory CD8 T-cell responses suggesting this as the mechanism for the bystander activation. These data have important implications for accurate assessment of immune responses generated by vaccines intended to [...]

Find the latest version:

<https://jci.me/124443/pdf>



**Bystander responses impact accurate detection of murine and human antigen-specific  
CD8 T cells**

Matthew D. Martin<sup>1</sup>, Isaac J. Jensen<sup>2</sup>, Andrew S. Ishizuka<sup>3</sup>, Mitchell Lefebvre<sup>2</sup>, Qiang Shan<sup>4</sup>,  
Hai-Hui Xue<sup>2,4,5</sup>, John T. Harty<sup>1,2,4</sup>, Robert A. Seder<sup>3</sup>, and Vladimir P. Badovinac<sup>1,2,4</sup>

<sup>1</sup>Department of Pathology, University of Iowa, Iowa City, Iowa, USA. <sup>2</sup>Interdisciplinary Graduate  
Program in Immunology, University of Iowa, Iowa City, Iowa, USA. <sup>3</sup>Vaccine Research Center,  
National Institute of Allergy and Infectious Diseases, National Institutes of Health, Bethesda,  
Maryland, USA. <sup>4</sup>Department of Microbiology and Immunology, University of Iowa, Iowa City,  
Iowa, USA. <sup>5</sup>Iowa City Veterans Affairs Health Care System, Iowa City, IA 52246

The authors have declared that no conflict of interest exists

Correspondence should be addressed to:

Vladimir Badovinac; (319)-384-2930; [vladimir-badovinac@uiowa.edu](mailto:vladimir-badovinac@uiowa.edu); The University of Iowa, 3-  
550 Bowen Science Building, Iowa City, IA 52242

Robert Seder; (301)-594-8483; [rseder@mail.nih.gov](mailto:rseder@mail.nih.gov); 40 Convent Drive, Bldg. 40, Rm. 3512,  
Bethesda, MD 20814

**Abstract**

Induction of memory CD8 T cells is important for controlling infections such as malaria HIV/AIDS, and for cancer immunotherapy. Accurate assessment of antigen (Ag)-specific CD8 T-cells is critical for vaccine optimization and defining correlates of protection. However, conditions for determining Ag-specific CD8 T-cell responses ex-vivo using ICS may be variable, especially in humans with complex antigens. Here, we used an attenuated whole parasite malaria vaccine model in humans and various experimental infections in mice to show that the duration of antigenic stimulation and timing of brefeldin A (BFA) addition influences the magnitude of Ag-specific and bystander T cell responses. Indeed, following immunization with an attenuated whole sporozoite malaria vaccine in humans, significantly higher numbers of IFN- $\gamma$  producing memory CD8 T-cells comprised of antigen specific and bystander responses were detected by increasing the duration of Ag-stimulation prior to addition of BFA. Mechanistic analyses of virus-specific CD8 T-cells in mice revealed that the increase in IFN- $\gamma$  producing CD8 T-cells was due to bystander activation of Ag-experienced memory CD8 T-cells, and correlated with the proportion of Ag-experienced CD8 T-cells in the stimulated populations. Incubation with anti-cytokine antibodies (ex. IL-12) improved accuracy in detecting *bona-fide* memory CD8 T-cell responses suggesting this as the mechanism for the bystander activation. These data have important implications for accurate assessment of immune responses generated by vaccines intended to elicit protective memory CD8 T-cells.

## Introduction

CD8 T cells have a role in mediating protection in humans against diverse pathogens impacting public health such as HIV, influenza, and *Plasmodium*, the causative agent of malaria, and tumors (1-5). The critical factors for mediating protective immunity by T cells include the magnitude, quality, breadth, and location. Indeed, subjects with greater numbers of memory CD8 T cells are better protected against infection (6, 7). Therefore, the development of preventive and therapeutic vaccines against infections and tumors requires a precise understanding of how to generate and accurately assess CD8 T cell responses.

There are now a variety of techniques to measure CD8 T cell responses, each with strengths and weaknesses. Peptide-MHC tetramer staining allows for an accurate enumeration of epitope-specific cells within the host and the evaluation of their phenotypic traits, but provides limited information on the functionality of the T cell response. Additionally, peptide-MHC tetramer analyses require knowledge of both the exact T cell epitope and MHC allele, which vary considerably between individuals, making assessment of the antigenic breadth of response resource intensive. Antigen-stimulated detection of T cells by ICS, in contrast, allows for assessment of T cell responses in an MHC agnostic manner since stimulation of T cells occurs through autologous antigen (Ag) presentation. However, a limitation of the ICS assay, in which overlapping peptides are often used to stimulate T cells, is that the exact T cell epitope is not determined, and thus, the breadth of the host responses is not as precisely defined.

Additionally, while ICS assays can provide data on the functional and phenotypic traits of responding cells, cells typically require stimulation for greater than 6 hours, during which time the cell phenotype of activated cells may change.

While alternative methods for detecting Ag-specific cells are used by some groups, such as activation-induced expression of CD137 (8), IFN- $\gamma$  is the canonical gold-standard cytokine for

ICS-based enumeration of Ag-specific CD8 T cells. In a review of the literature, we determined that methods of conducting ICS, including length of incubation and timing of BFA (a golgi-disrupting compound used to prevent secretion of cytokines) addition, vary widely. Most often, ICS stimulation occurs for between 5 and 24 hours, and BFA is added several hours after the beginning of stimulation (4, 6, 9-39). While delaying addition of BFA may be necessary with certain types of antigen stimulations such as using whole pathogens rather than peptides to allow for Ag processing and presentation on MHC needed to drive cytokine production by CD8 T cells, delayed BFA addition may also allow for the release of cytokines into the culture media if using stimuli that have innate stimulatory activity. Inflammatory cytokines such as IL-12 could enhance IFN- $\gamma$  production by Ag-specific CD8 T cells that respond to antigens used for stimulation, but also by memory T cells that are specific for other antigens (bystander activation). This is supported by evidence that Ag-experienced effector or memory CD8 T cells can be induced to produce IFN- $\gamma$  not only in response to cognate Ag, but also in a bystander manner that is solely driven by inflammatory cytokines (40-42). Thus, we sought to understand how variations in the conditions of ICS impact the accurate accounting of infection- or vaccine-induced Ag-specific CD8 T cells. These data have implications for improving vaccine design and accurately assessing correlates of CD8 T cell mediated protection.

## Results

### **The frequency of IFN- $\gamma$ producing CD8 T cells detected in humans following vaccination is increased with increased time of ex-vivo Ag stimulation**

The potency and protective capacity of a vaccine can be evaluated partly based upon the magnitude of the induced memory CD8 T cell population. To begin to address the impact of varying the assay conditions on enumeration of Ag-specific CD8 T cell memory, we assessed the frequency of Ag-specific memory CD8 T cells following vaccination of human subjects with

an attenuated whole sporozoite malaria vaccine (4, 6, 43). Employing a peptide stimulation assay for this vaccine would be technically challenging due to MHC polymorphism and the large number (>2000) of potential antigens presented to the immune system. Therefore, we utilized a previously developed assay where stimulation of CD8 T cells was achieved by incubating PBMCs from vaccinated subjects with the vaccine itself, which consists of aseptic, purified, irradiated, metabolically-active *Plasmodium falciparum* sporozoites (PfSPZ), and where 12-hour stimulation was more sensitive than 6-hour stimulation (4). Here, we extended these data and incubated PBMCs from a vaccinated or nonimmunized subject with PfSPZ for 12, 16, 20, and 24 hours, with BFA being added for the final four hours. While the nonimmunized subject had no IFN- $\gamma$  production above background for the duration of stimulation, the percentage of CD8 T cells that produced IFN- $\gamma$  in the PfSPZ-vaccinated subject increased substantially over time (Figure 1A), suggesting that duration of ICS increased the detection of total IFN- $\gamma$  producing CD8 T cells.

Addition of BFA is used in ICS assays to block release of IFN- $\gamma$  within the T cell, thereby improving the sensitivity of the response. However, BFA also could inhibit efficient Ag-processing and presentation of PfSPZ (44). To determine if timing of BFA addition impacted the detection of IFN- $\gamma$  producing CD8 T cells, cells were stimulated with PfSPZ for a total of 24 hours, with BFA being added after the first 8, 16, or 20 hours of incubation. A substantially higher percentage of CD8 T cells producing IFN- $\gamma$  was detected when BFA was added 16 or 20 hours after beginning stimulation (Figure 1B), indicating that the timing of BFA addition strongly influences the frequency of IFN- $\gamma$  producing CD8 T cells detected.

Delayed addition of BFA would allow for soluble factors including inflammatory cytokines to be released into the culture, and potential bystander activation of Ag-experienced effector and memory CD8 T cells. Thus, it is unclear if enhanced detection of IFN- $\gamma$  producing CD8 T cells observed by increasing incubation time or by delaying addition of BFA was due to

increased sensitivity in detecting *Plasmodium*-specific CD8 T cells, and/or by triggering IFN- $\gamma$ -production by non-malaria Ag-experienced CD8 T cells.

### **Delayed addition of BFA leads to bystander activation of Ag-experienced CD8 T cells**

To further determine how ICS conditions altered detection of Ag-specific CD8 T cells, we used a well-defined mouse model that allows precise detection of CD8 T cells of known Ag-specificity. Mice (B6, Thy1.2) received adoptive transfer of naïve TCR-transgenic GP<sub>33</sub>-specific P14 cells (Thy1.1), before LCMV-Armstrong infection (Figure 2A), and memory P14 cells were detected by Thy1.1 expression. Additionally, infection of B6 mice with LCMV elicits large Ag-specific CD8 T cell responses that recognize LCMV-derived GP<sub>33</sub> and NP<sub>396</sub> epitopes (45), and we used peptide stimulated ICS to detect cytokine producing memory CD8 T cells responding to GP<sub>33</sub> and NP<sub>396</sub> peptides (Figure 2B-D). Mice generated in this manner contain endogenous (Thy1.1 neg- blue gates) CD8 T cells that consist of naive cells and Ag-specific cells that recognize GP<sub>33</sub> and NP<sub>396</sub> epitopes as well as additional LCMV-derived epitopes, and Ag-experienced P14 cells (Thy1.1 pos- red gates) that recognize GP<sub>33</sub>, but not NP<sub>396</sub> peptides. Addition of P14 cells allows for detection of true Ag-specific responses (in response to GP<sub>33</sub> peptide) and bystander responses (in response to NP<sub>396</sub> peptide), while IFN- $\gamma$  production by endogenous CD8 T cells, due to mixed epitope specificities of this population, could represent either true Ag-specific responses or responses that include both Ag-specific and bystander responses. To highlight this, as can be seen in Figure 2B-D, we present detection of IFN- $\gamma$  producing cells following ICS gated on total lymphocytes (lymphocyte gate), total CD8 T cells with identification of endogenous (blue gates) or P14 (red gates) cells based on Thy1.1 expression (CD8 gate), or total P14 cells (Thy1.1+/CD8+ (P14) gate).

Of note, since detection of IFN- $\gamma$  producing CD8 T cells is impacted by peptide concentration and number of cells plated, we first identified conditions that allow for maximal detection of *bona fide* Ag-specific CD8 T cells (ex.  $2 \times 10^6$  cells/well and 200 nm peptide concentration) (Supplemental Figure 1, A and B). Inflammatory cytokines can potentially cause bystander activation of Ag-experienced CD8 T cells when BFA is not present during the entire incubation (40-42, 46), so we first sought to determine if timing of BFA addition impacted detection of IFN- $\gamma$  producing CD8 T cells following specific peptide stimulation. Interestingly, between a ~1.5- to 2-fold increase in the percentage of endogenous CD8 T cells producing IFN- $\gamma$  in response to GP<sub>33</sub> or NP<sub>396</sub> peptide was observed when BFA was added for the last hour (7+1) compared to when it was present during the entire incubation (0+8) (Figure 2, B-D CD8 gate - blue boxes and Figure 2E). Similar results were observed for LCMV immune mice that did not receive P14 cells (Supplemental Figure 1, C and D).

A similar percentage of P14 cells produced IFN- $\gamma$  following GP<sub>33</sub> peptide stimulation regardless of timing of BFA addition (Figure 2C P14 gate), suggesting that delayed addition of BFA does not impact IFN- $\gamma$  production of *bona fide* Ag-specific CD8 T cells. To determine whether increases in IFN- $\gamma$  producing CD8 T cells that occurred with delayed BFA addition were due to bystander activation, we examined responses of 'sensor' GP<sub>33</sub>-specific Thy1.1 P14 cells in response to NP<sub>396</sub> peptide stimulation. While few IFN- $\gamma$  producing P14 cells were detected following stimulation with NP<sub>396</sub> peptide in the presence of BFA for the entire incubation, 25-30% of memory P14 cells produced IFN- $\gamma$  in response to NP<sub>396</sub> peptide when BFA was not present during the whole incubation time (Figure 2D red boxes). Analyses of T cell responses by ICS in human samples often rely on stimulation for greater than 8 hours, with addition of BFA before the last hour of incubation. To determine if bystander responses contribute to IFN- $\gamma$  producing cells detected for incubation times of greater length and when BFA is added earlier in the



culture, we stimulated splenocytes from LCMV immune mice that contained memory P14 cells with NP<sub>396</sub> peptide for 8 hours and added BFA after 4 or 7 hours, or for 12 hours and added BFA after 4, 8, or 11 hours. Bystander responses by P14 cells could be detected when BFA was added prior to the last hour and when cells were stimulated for 8 or more hours, and bystander responses increased with greater length of stimulation in the absence of BFA (Supplemental Figure 2). Thus, delayed addition of BFA in both the mouse and human models of viral and malaria specific CD8 T cells can result in bystander activation of Ag-experienced CD8 T cells leading to inflation in frequencies and numbers of Ag-specific CD8 T cells detected.

#### **Contribution of bystander IFN- $\gamma$ activation is dependent upon CD8 T cell pool composition and length of stimulation**

Ag-experienced CD8 T cells can undergo bystander activation and produce cytokines such as IFN- $\gamma$  while naïve CD8 T cells cannot (40, 46). Of note, the representation of Ag-experienced cells within the CD8 T cell pool for human subjects can vary widely based on age and history of previously encountered infections (47, 48). To determine whether the composition of Ag-experience in the CD8 T compartment dictated frequencies of IFN- $\gamma$  producing CD8 T cells, we manipulated the number of Ag-experienced cells among splenocytes by mixing splenocytes from LCMV-immune mice with graded numbers of sorted memory P14 'sensor' cells to achieve different ratios of naïve (CD11a low/CD8 hi) to memory (CD11a hi/CD8 low) CD8 T cells (49, 50) (Figure 3, A and B). Again, few IFN- $\gamma$  producing P14 cells were detected following stimulation with NP<sub>396</sub> peptide when BFA was present for the entire incubation, and a similar percentage of CD8 T cells producing IFN- $\gamma$  in response to NP<sub>396</sub>-peptide stimulation was observed regardless of numbers of P14 cells present (Figure 3, C and D, (0+8 group)). However, when BFA was not present for the entire incubation, the percentage of IFN- $\gamma$  producing CD8 T cells in response to NP<sub>396</sub>-peptide stimulation increased with increasing

197 numbers of 'sensor' P14 cells, and this was due to increased representation of P14 cells rather  
198 than elevation in the frequency of activated bystander P14 cells (Figure 3, C and D, (7+1  
199 group)). Thus, the contribution of bystander activated cells to the IFN- $\gamma$  producing CD8 T cell  
200 population was dependent upon the representation of Ag-experienced cells within the CD8 T  
201 cell compartment. These data suggested that the increase in the frequency of vaccine targeted  
202 memory CD8 T cells might be more pronounced in older subjects and/or subjects with  
203 substantial history of pathogen exposures that possess more previously activated CD8 T cells.

204  
205 The duration of antigen-stimulation *ex vivo* for experiments involving human subjects varies, but  
206 in most instances stimulation times are between 5 and 24 hours (4, 6, 9-39). To determine if the  
207 duration of stimulation contributed to the degree of bystander IFN- $\gamma$  detected when BFA is not  
208 present for the entire incubation, splenocytes from an LCMV immune mouse were incubated  
209 with GP<sub>33</sub> or NP<sub>396</sub> peptides for 5, 8, 16, or 24 hours with BFA present for the entire incubation or  
210 for the final hour of incubation. Regardless of length of incubation, a greater percentage of  
211 IFN- $\gamma$  producing CD8 T cells was detected following stimulation with GP<sub>33</sub> (Figure 4, A and B) or  
212 NP<sub>396</sub> (Figure 4, C and D) peptides when BFA was added for only the last hour of incubation.  
213 However, increased detection of IFN- $\gamma$  producing CD8 T cells was most pronounced when  
214 samples were incubated for greater than 5 hours. Similarly, bystander activated P14 cells were  
215 detected in response to NP<sub>396</sub>-peptide stimulation when BFA addition was delayed for any  
216 length of incubation tested, but percentages of bystander activated P14 cells detected were  
217 greater when samples were incubated for greater than 5 hours (Figure 4E). These data  
218 suggested that bystander activation occurred and contributed to the frequency of IFN- $\gamma$   
219 producing CD8 T cells detected when BFA is not present for the entire incubation across the  
220 spectrum of incubation times used to conduct ICS. However, contribution of bystander activated  
221 cells to IFN- $\gamma$  producing cells detected is likely to increase with greater lengths of incubation.

**Delayed addition of BFA leads to bystander activation of Ag-experienced CD8 T cells following stimulation with whole pathogen**

Application of peptide-stimulated ICS assays across individual human subjects assessing responses to complex pathogens with many antigens is difficult due to differences in HLA haplotype, thus, stimulation of human samples is often achieved by exposing samples to whole pathogens (Figure 1), or through the use of libraries of long overlapping peptides, methods that may require a period of BFA-free culture to allow for optimal Ag processing and presentation or cross presentation. To determine if bystander activated cells contributed to the frequency of IFN- $\gamma$  producing cells detected after stimulation with whole pathogens, splenocytes from an LCMV immune mouse ('sensor' cells) were incubated with CFSE labeled splenocytes that were either pulsed with GP<sub>33</sub> peptide or infected with VacV expressing cognate Ag (VacV-GP<sub>33</sub>) or an irrelevant Ag (VacV-OVA) (Figure 5A). When BFA was present throughout the incubation period, IFN- $\gamma$  production from the LCMV immune sensor cells was observed in response to spleen cells pulsed with GP<sub>33</sub> peptide or infected with VacV-GP<sub>33</sub> and the percentage of IFN- $\gamma$  producing CD8 T cells detected increased with increasing numbers of stimulator cells added to the culture (Figure 5B). IFN- $\gamma$  production was not observed in response to splenocytes infected with VacV-OVA (Figure 5C, bottom).

Interestingly, an increased percentage of IFN- $\gamma$  producing sensor cells were detected following incubation with greater numbers of GP<sub>33</sub> pulsed or VacV-GP<sub>33</sub> infected stimulator cells and when addition of BFA was delayed for longer periods (Figure 5C top and middle). These data suggested that length of incubation with BFA impacted detection of IFN- $\gamma$  producing CD8 T cells following stimulation with pathogen infected splenocytes. However, because we could not determine if our stimulation conditions resulted in IFN- $\gamma$  production by bona fide Ag-specific or

any Ag-experienced CD8 T cells, we were unable to conclude if delayed addition of BFA resulted in increased detection of true Ag-specific CD8 T cells, or if increased percentages of IFN- $\gamma$  producing CD8 T cells detected was due to bystander activation of memory CD8 T cells. To address this, we incubated sensor cells from LCMV P14 chimera immune mice with stimulator cells that were either pulsed with NP<sub>396</sub> peptide or infected with VacV expressing LCMV nucleoprotein (VacV-NP). An increased percentage of IFN- $\gamma$  producing cells was detected following stimulation with peptide pulsed or VacV-NP infected cells when BFA was not present for the whole incubation time (Figure 5, D and E). Importantly, in the same samples, GP<sub>33</sub>-specific P14 memory CD8 T cells produced IFN- $\gamma$  in response to VacV-NP infected splenocytes, strongly suggesting antigen-independent bystander activation. Thus, stimulation with whole pathogens, while not as potently as peptide-stimulation, also resulted in bystander CD8 T cell activation, and the potential for inaccurate accounting of pathogen/vaccine specific CD8 T cell responses.

### **Blocking inflammatory cytokines limits bystander activation of CD8 T cells**

Bystander IFN- $\gamma$  production by effector or memory CD8 T cells can be stimulated by hundreds of inflammatory cytokine combinations (42). As an example, a large percentage of endogenous and P14 memory CD8 T cells derived from LCMV immune P14 chimera mice produced IFN- $\gamma$  in response to IL-12 and IL-18, IL-12 and TNF- $\alpha$ , or IL-12 and IL-15 stimulation alone, but only when BFA was not present during the entire incubation (Figure 6A and Supplemental Figure 3 A and B). Similarly, addition of IL-12 and IL-18 significantly increased the frequency of IFN- $\gamma$  producing CD8 T cells even in the presence of peptide (GP<sub>33</sub> – Fig 6B; NP<sub>396</sub> – Figure 6C) stimulation, but only if BFA addition was delayed. Of note, addition of IL-12 and IL-18 (one of the most potent cytokine combinations that leads to bystander activation) (42) did not increase the number of peptide stimulated IFN- $\gamma$  producing cells (GP<sub>33</sub> or NP<sub>396</sub> – Figure 6D) if BFA was

present all the time (0+8 group). Furthermore, as described previously, human PBMCs incubated with IL-12 and IL-18 also produced IFN- $\gamma$  (51-53), but only when BFA was not present during the entire incubation (Supplemental figure 3 C and D). This suggested that human samples also may be susceptible to inflammation-driven bystander responses, similar to those observed in mice during ICS when BFA is not present for the entire incubation. Thus, accurate detection of Ag-specific human CD8 T cells by ICS may be influenced by timing of BFA addition.

These data also suggest that bystander responses elicited in response to Ag-stimulation when BFA is not present in culture for the entire incubation require intact golgi function. Two possible explanations for the absence of bystander responses in the presence of BFA for the entire culture, then, are 1) that BFA prevents cytokine secretion that elicits bystander responses, or 2) that BFA prevents transport of cytokine receptors to the cell surface, blocking the ability of cells to respond to inflammatory cues. It is also possible that both mechanisms contribute to bystander responses elicited when addition of BFA is delayed. Data presented in Figure 2 and Supplemental Figure 3 suggests that cytokines secreted in response to cognate Ag can drive bystander responses when addition of BFA is delayed, as adding non-cognate Ag alone is able to induce bystander responses (7+1, Thy1.1+/CD8+ (P14) gates). Additionally, when we analyzed expression of cytokine receptor components we found that transcript levels of *Il12rb2*, a signaling component of the IL-12 receptor complex that activates STAT4 signaling and whose expression is regulated by inflammatory cytokines (54), and *Tnfrs1b*, which binds TNF $\alpha$  and activates NF- $\kappa$ B and MAPK pathways (55), were increased in sorted P14 cells that were activated in a bystander manner in ICS cultures stimulated with NP<sub>396</sub> peptide where addition of BFA was delayed (Supplemental Figure 4, A and B). Transcript levels of *Ifngr1* and *Ifngr2*, which bind IFN- $\gamma$  and activates STAT1 pathways (56), were not impacted by delayed addition of

BFA in P14 cells (Supplementary Figure 4B), suggesting that the absence of BFA does not sensitize cells capable of undergoing bystander responses to IFN- $\gamma$  mediated signaling. However, since IFN- $\gamma$  receptors are expressed on the surface of nearly all cells, IFN- $\gamma$  may be acting on other cells in ICS cultures that play a role in driving bystander responses. Thus, delayed addition of BFA during ICS is likely to elicit bystander responses through the combinatorial effects of allowing for secretion of inflammatory cytokines that drive bystander responses into culture media, and by allowing for export of inflammatory cytokine receptors to the surface of Ag-experienced cells, which enhances sensitivity to inflammatory cytokines.

A further suggestion from the data presented in Figure 6 is that cytokine blockade during stimulation could enhance the fidelity of detecting bone fide antigen-specific CD8 T cells by the ICS assay. To test this, splenocytes from LCMV chimera P14 mice were incubated with NP<sub>396</sub> peptide for 8 hours in the presence of BFA for the entire incubation or for the final hour, with or without anti-IL-12, -IFN- $\gamma$  and/or -TNF- $\alpha$  blocking Abs. While incubation of splenocytes in the absence of BFA led to bystander IFN- $\gamma$  production and increased percentages of IFN- $\gamma$  producing CD8 T cells, addition of a cocktail of cytokine blocking Abs was maximally effective at limiting bystander responses, and addition of blocking Abs to individual cytokines, to varying degrees, reduced the percentages of endogenous (Figure 7A) or P14 cells (Figure 7B) producing IFN- $\gamma$  in a bystander manner, thus improving the overall accuracy in detecting Ag-specific memory CD8 T cells. In summary, these data suggest that blocking inflammatory cytokines during stimulation can reduce the contribution of bystander activated cells to IFN- $\gamma$  producing Ag-specific CD8 T cells detected by ICS, and may provide for a more accurate estimation of Ag-specific CD8 T cells using different ICS protocols.

**Bystander activated human CD8 T cells contribute to IFN- $\gamma$ -producing cells detected following stimulation with whole pathogens**

The data in Figure 5 from the mouse model showed that stimulation with whole pathogens could lead to bystander activation of CD8 T cells, and the data in figure 1 from humans showed that there was a higher percentage of IFN- $\gamma$  producing cells detected in PfSPZ vaccinated human subjects following ICS of longer duration and when BFA was added later in the stimulation. To determine if bystander activation of CD8 T cells contributed to the pool of IFN- $\gamma$  producing CD8 T cells detected in human subjects, PBMCs from PfSPZ- vaccinated subjects were labeled with CFSE and individually combined at a ratio of 9:1 with PBMCs obtained from the same subjects prior to vaccination (Figure 8A). This design allows for detection of bystander responses, as any IFN- $\gamma$  producing cells in the pre-vaccine population of cells could only be due to non-cognate Ag driven responses. Cells were then incubated with PfSPZs for 12, 16, or 20 hours in the presence of BFA for the last 4 hours. While IFN- $\gamma$  producing CD8 T cells were low to undetectable when pre-vaccine PBMCs were cultured in the absence of post-vaccine PBMCs, a significant percentage of pre-vaccine PBMCs produced IFN- $\gamma$  when cultured with post-vaccination PBMCs (Figure 8B). These data showed that, under conditions of stimulation used most commonly for detection of CD8 T cells by the ICS assay from subjects that receive whole sporozoite vaccine (57, 58), bystander activation of human CD8 T cells can confound the enumeration of bona fide pathogen/vaccine induced memory CD8 T cells.

Of note, design of whole pathogen stimulation assays for mice shown in figure 5, where infection of stimulator splenocytes occurred prior to mixing with sensor cells of interest, was different than for the human assays shown in figure 8, where whole pathogen was added directly to cells of interest at the initiation of culture. To determine if bystander responses in mice following whole pathogen stimulation also contributed to IFN- $\gamma$  producing cells detected when whole pathogens were added directly to samples being analyzed, we designed

experiments shown in Supplemental Figure 5A and D. With two different models, activation of P14 cells following stimulation with bacterium *Listeria monocytogenes* (LM-OVA/B8R) (Supplemental Figure 5B) and activation of OT-I cells following stimulation with Vaccinia virus (VacV-GP<sub>33</sub>) (Supplemental Figure 5E), bystander responses contributed to IFN- $\gamma$  producing cells detected. Furthermore, addition of cytokine blocking Abs reduced the contribution of bystander P14 responses detected (Supplemental Figure 5C).

Additionally, to determine if bystander responses in mice influenced evaluation of CD8 T cell responses elicited following experimental malaria vaccination, we performed ICS using GAP50 peptide, which is a *Plasmodium berghei*-derived epitope for which naïve B6 mice possess a large Ag-specific naïve CD8 T cell repertoire (59), with splenocytes from mice that were inoculated with radiation attenuated *Plasmodium berghei* sporozoites, and that contained memory P14 cells generated in response to prior infection with LCMV (Supplemental Figure 6A). The size of the CD8 T cell response detected, and contribution of bystander activated cells to IFN- $\gamma$  producing cells detected increased with increasing length of incubation in the absence of BFA (Supplemental Figure 6 B and C). Thus, modified mouse models recapitulate the findings observed with human cells, suggesting that bystander responses can contribute to IFN- $\gamma$  producing cells detected when addition of BFA is delayed.

Lastly, to determine if addition of cytokine blocking Abs may be useful in limiting contribution of bystander responses to human Ag-specific CD8 T cells detected by ICS when addition of BFA is delayed, we performed ICS with human PBMCs obtained at the University of Iowa DeGowen Blood Center using peptide pools containing cytomegalovirus (CMV) and Epstein-Barr virus (EBV) derived epitopes. Percentages of IFN- $\gamma$  producing cells detected were elevated when addition of BFA was delayed (Supplemental Figure 7A and B- black dots compared to white dots), suggesting that bystander responses were contributing to Ag-specific cells detected when BFA addition was delayed. However, percentages of IFN- $\gamma$  producing cells



detected were not significantly different between samples incubated in the presence of BFA from the beginning of stimulation and for samples for which addition of BFA was delayed but for which cytokine blocking Abs were added to ICS cultures (Supplemental Figure 7A and B- black dots compared to red dots). These data suggest that addition of cytokine blocking Abs during ICS may be useful for accurate assessment of numbers of true Ag-specific human CD8 T cells when using ICS.

## Discussion

The frequency and phenotype of Ag-specific memory CD8 T cells present prior to infection impact the host's ability to fight pathogenic microorganisms. Therefore, accurately identifying Ag-specific memory CD8 T cells generated in response to vaccination will facilitate vaccine development, for example, through accurate assessment of the immune correlates of protection. Additionally, assays that seek to further characterize the CD8 T cell response, for example, by determining expression of phenotypic markers on IFN- $\gamma$ -producing cells by multi-parameter flow cytometry or by sorting activated cells and performing single-cell RNA sequencing, may be misled by incorrect identification of bona-fide Ag-specific CD8 T cells.

Here we have shown that, when using ICS to detect CD8 T cell responses, bystander activation of Ag-experienced CD8 T cells can occur when BFA is not present for the entire period of stimulation. Bystander activation was seen in both mouse and human models of viral and malaria infection as well as bacterial infection in mice, and was influenced by the length of stimulation with peptides and whole pathogens. Of note, the contribution of bystander activated cells to the IFN- $\gamma$  producing CD8 T cell population depended on the frequency of Ag-experienced CD8 T cells in the sample. Thus, the over-representation of Ag-specific CD8 T cells when ICS is performed without BFA for the entire incubation period will vary depending on the

individual examined. However, delaying addition of BFA in human samples may be unavoidable when the antigen sources are whole pathogens/proteins that require undisrupted cell machinery for efficient antigen processing and presentation or cross presentation. In these cases, addition of cytokine blocking Abs to ICS cultures may aid in minimizing bystander responses and result in greater accuracy for detection of true Ag-specific responses.

This study does have limitations. There are a number of additional parameters that may vary in ICS protocols that have the potential to impact readout of IFN- $\gamma$  producing cells detected such as number of T cells in culture, representation of Ag-presenting cells, media used, and instrumentation. This is not an exhaustive list, and we were unable to test the impact of every parameter on ICS readout. Furthermore, while we did examine a number of different incubation lengths and timings of BFA addition, we did not exhaustively test how length of incubation and timing of BFA addition impact bystander activation during ICS culture. We were able to detect bystander responses across a range of incubation times from 5 to 24 hours with addition of BFA as early as 4 hours after initiation of ICS (Figure 4 and Supplemental Figure 2). However, bystander responses became magnified with incubations of greater length and with addition of BFA at later times after onset of culture. Thus, choosing incubation times of shorter duration with addition of BFA at earlier times, when allowed for based on nature of stimulation, may be an additional method to improve accuracy in detection of true Ag-specific responses by ICS.

If ICS assay is providing inaccurate estimates of memory CD8 T cells present within the host, are other techniques available that might provide a more accurate estimate? An alternative assay for measuring Ag-specific T cell responses, the ELISpot assay, is similarly compromised by bystander activation. While ELISpot is generally considered to be more sensitive than ICS, and thus better-suited for detection of rare Ag-specific cells (60), like ICS, it relies on detection of IFN- $\gamma$  producing CD8 T cells following incubation with cognate peptide. Additionally, ELISpot

assays commonly have incubation periods lasting for 18-48 hours, and such long incubation periods are likely to further exacerbate the bystander activation phenomenon.

Peptide-MHC tetramer staining is also used to measure Ag-specific T cell responses. Unlike ICS conducted following stimulation with antigenic peptide pools or whole pathogens, tetramer staining must be tailored to individual subjects due to differences in MHC haplotypes among individuals (61). Therefore, it can be more logistically challenging than ICS, especially for complex pathogens with thousands of proteins such as malaria, which can be performed similarly in disparate hosts. Furthermore, tetramer staining marks Ag-specific cells with limited information about cell functionality. Following ICS with GP<sub>33</sub> peptide, only ~80% of P14 cells that are known to recognize the GP<sub>33</sub> epitope of LCMV responded with IFN- $\gamma$  production (Figures 2 and 6), suggesting that some memory cells within the host are not capable of performing effector functions. At least some of these cells are likely to be T<sub>DIM</sub> cells, which are generated during the process of homeostatic memory cell turnover, and are incapable of IFN- $\gamma$  production or release of cytotoxic granules (62). Because host protection is ultimately dependent upon the number of cells present that are capable of responding to invading microbes with effector functions, ICS may provide a more accurate measure of protection than tetramer staining, as the former detects only cells capable of executing effector functions, while the latter detects cells that may be non-functional.

How can ICS be tailored to provide a more accurate assessment of Ag-specific CD8 T cell responses? Reductions in bystander activation can be achieved by selecting the shortest possible length of incubation and by adding BFA at the beginning of stimulation. However, when inclusion of BFA at the onset of ICS is not feasible due to stimulation with whole pathogen or proteins that require processing, additional steps can be performed to reduce bystander

activation and provide a more accurate enumeration of bona fide Ag-specific CD8 T cells. The severity of bystander activation can be mitigated by allowing pathogen processing and presentation to proceed first in a pure culture of antigen-presenting cells prior to the concurrent addition of syngeneic T cells and BFA. If such a strategy is not feasible, blocking antibodies to cytokines detected in the supernatant could be added during incubation to reduce bystander activation and increase accuracy.

Taking these steps to ensure accurate detection of Ag-specific effector or memory CD8 T cells will likely aid in evaluation and design of vaccines for infections of global importance and for cancer immunotherapy.

## **Methods**

### **Human subjects, PfSPZ vaccination, and collection of PBMCs**

Human samples from malaria vaccinated or naïve subjects were obtained from the VRC 314 study, as described (63). Briefly, healthy US adult volunteers were vaccinated intravenously with the PfSPZ Vaccine (64). EDTA-anti-coagulated whole blood was collected prior to vaccination and after the final vaccination. PBMCs were isolated by density gradient centrifugation and cryopreserved in LNVP.

### **Mice, infections, and generation of memory CD8 T cells**

Inbred female C57Bl/6 mice were purchased from the National Cancer Institute (Frederick, MD) and bred at the University of Iowa, and TCR Tg P14 and OT-I mice were bred at the University of Iowa. All mice were used at 6-10 weeks of age and housed at the University of Iowa at appropriate biosafety levels.

All LCMV Armstrong infections were performed intraperitoneally with  $2 \times 10^5$  plaque forming units (PFU) per mouse. All *Listeria monocytogenes* (LM) infections were performed intravenously (i.v.- retroorbital injection) with  $1 \times 10^7$  colony forming units (CFU) per mouse of attenuated (Att) LM expressing the OVA<sub>257</sub> peptide and the full length B8R protein from Vaccinia virus (VacV) (LM-OVA/B8R). For infections with radiation attenuated *P. berghei* sporozoites (Pb-RAS), *P. berghei* ANKA clone 234 sporozoites were isolated from the salivary glands of *A. stephensi* mosquitos purchased from the insectary of New York University. Sporozoites were attenuated by radiation with 200 Gray (Gy) by cesium irradiation prior to i.v. (retroorbital) injection of  $2 \times 10^4$  sporozoites per mouse. In vitro infections were performed using VacV expressing the OVA<sub>257</sub> peptide (VacV-OVA), the GP<sub>33</sub> peptide (VacV-GP<sub>33</sub>), or the full-length nuclear protein (NP) from LCMV (VacV-NP; obtained from Dr. Steven Varga, Department of Microbiology and Immunology, University of Iowa, Iowa City, Iowa), or LM-OVA/B8R expressing the full-length OVA peptide and B8R peptide derived from VacV (Obtained from JD Sauer, Department of Medical Microbiology and Immunology, University of Wisconsin, Madison, Wisconsin).

1° memory P14 cells were generated by adoptively transferring  $5 \times 10^3$  P14 cells obtained from peripheral blood of naïve P14 mice (Thy1.1/1.1 or Thy1.1/1.2) into naïve C57Bl/6 recipients (Thy1.2/1.2) followed by infection with LCMV. 1° memory OT-I cells were generated by adoptively transferring  $5 \times 10^3$  OT-I cells obtained from peripheral blood of naïve OT-I mice (Thy1.1/1.1 or Thy1.1/1.2) into naïve C57Bl/6 recipients (Thy1.2/1.2) followed by infection with LM-OVA/B8R.

#### ICS and flow cytometry for human and mouse samples

For figure 1,  $1.5 \times 10^6$  PBMCs from PfSPZ immunized or non-immunized (naïve) subjects were incubated with  $1.5 \times 10^5$  PfSPZs for the durations indicated. BFA (GolgiPlug™, BD Biosciences cat# 555029) was added to the culture medium at the times indicated at 10 µg/mL.

498

499 For figure 8, post vaccination PBMCs were CFSE labeled and mixed at a 9:1 ratio with pre-  
500 immunization PBMCs, and a total of  $1.5 \times 10^6$  PBMCs were incubated with  $1.5 \times 10^5$  PfSPZs for  
501 the times indicated, and with addition of BFA for the last 4 hours of incubation.

502

503 After stimulation, cells were stained as previously described (65). Briefly, cells were stained for  
504 viability with Aqua Live-Dead dye (Invitrogen), surface stained with CCR7 (clone Ax680, NIH  
505 vaccine research center), CD3 (clone SP34.2, BD), TCR- $\gamma\delta$  (clone B1, BD), CD4 (clone OKT4,  
506 BioLegend), CD8 (clone RPA-T8, BioLegend), CD45RA (clone MEM-56, Invitrogen), and  
507 stained intracellularly for IFN- $\gamma$  (clone 4S.B3, BioLegend), IL-2 (clone MQ1-17H12, BioLegend),  
508 and TNF- $\alpha$  (clone Mab11, BioLegend). Flow cytometry data was acquired using a modified  
509 LSR-II (BD) and analyzed using FlowJo v9.9.6 (Tree Star Inc., Ashland, OR).

510

511 For human PBMCs examined in supplementary figures 3 and 7, LRS cones from a Trima Accel  
512 automated blood collection system (Terumo BCT, Lakewood, CO) were used to remove  
513 PBMCs, and the LRS cones were provided to investigators at the University of Iowa by the  
514 DeGowin blood center. PBMCs from cones were flushed by washing with complete RPMI  
515 followed by red blood cell lysis with ACK lysis buffer. PBMCs were then washed three times with  
516 complete RPMI and filtered through a 70 micron cell strainer before being resuspended in  
517 freezing media (90% Fetal Bovine Serum and 10%DMSO) and storage at  $-80^{\circ}\text{C}$ . Cells were  
518 revived from frozen stocks by being thawed in a water bath followed by suspension in warmed  
519 complete media. Cells were then washed 3 times in warmed media and strained through a 70  
520 micron cell strainer before  $2 \times 10^6$  cells were plated and incubated. For supplementary figure 3,  
521 cells were incubated with or without 100ng/mL human rIL-12 (BD Pharmingen) and IL-18  
522 (Medical and Biological laboratories) for a total of 8 hours with BFA present the entire incubation

(0+8) or for the final hour (7+1), or for a total of 20 hours with BFA present the entire incubation (0+20) or for the final four hours (16+4). For supplementary figure 7, cells were incubated with or without 200nM concentrations of peptide pools consisting of CMV pp50 peptide (VTEHDTLLY- presented by HLA-A\*0101 allele), CMV pp65 peptide (NLVPMVATV- presented by HLA-A\*0201 allele) and EBV BMLF-1 peptide (GLCTLVAMD- presented by HLA-A\*0201 allele) (all purchased from iba lifesciences), and with or without 0.6 µg/mL αIFN-γ, 0.6 µg/mL αTNF-α, 9 µg/mL αIL-12, and 9 µg/mL αIL-18 (all from R&D systems) for a total of 20 hours with BFA present the entire incubation (0+20) or for the final four hours (16+4). Cells were stained for surface expression of CD45RA (clone HI100, BioLegend), CD4 (clone A161A1, BioLegend), CD8 (clone HIT8a, BioLegend), and CD3 (clone HIT3a, BioLegend), and intracellular expression of IFN-γ (clone 4S.B3, BioLegend).

For mouse samples, spleens were collected and tissue was processed into single-cell suspension. Unless otherwise stated (Supplementary Figure 1),  $2 \times 10^6$  splenocytes were incubated with 200nM concentrations of GP<sub>33</sub>, NP<sub>396</sub>, or GAP50<sub>40</sub> peptide. Unless otherwise stated (Figures 4 and 5 and supplementary figures 2, 5, and 6), samples were incubated for a total of 8 hours with BFA present for the entire incubation (0+8) or for the final hour of incubation (7+1). In figure 4, cells were incubated for a total of 5, 8, 16, or 24 hours with BFA present for the entire incubation or for the final hour of incubation. In figure 5, cells were incubated for a total of 8 hours with BFA present for the entire incubation (0+8), for the final 6 hours of incubation (2+6), for the final four hours of incubation (4+4), or for the final hour of incubation (7+1). In supplemental figure 2, cells were incubated for a total of 8 hours with BFA present for the entire incubation (0+8), for the final four hours of incubation (4+4), or for the final hour of incubation (7+1), or for a total of 12 hours with BFA present for the entire incubation (0+12), for the final eight hours of incubation (4+8), for the final 4 hours of incubation (8+4), or for the final

hour of incubation (11+1). In supplemental figure 5, cells were incubated for a total of 12, 16, or 20 hours with BFA present for the final 4 hours of incubation. In supplemental figure 6, cells were incubated for a total of 12 hours with BFA present for the entire incubation (0+12), for the final eight hours of incubation (4+8), for the final 4 hours of incubation (8+4), or for the final hour of incubation (11+1).

In figure 3, P14 cells that were positively selected were added to splenocytes from an LCMV immune mouse prior to incubation. For positive selection, cells were stained with PE-anti-Thy1.1 antibodies (clone His51, eBioscience) and purified with anti-PE magnetic bead sorting using standard AutoMacs protocols.

In figure 6, splenocytes were incubated with or without 10ng/mL rIL-12 and IL-18 (R & D systems) in the presence or absence of 200nM GP<sub>33</sub> or NP<sub>396</sub> peptide. In supplementary figure 3, splenocytes were incubated with or without NP<sub>396</sub> peptide or with or without rIL-12 and IL-18, IL-12 and TNF- $\alpha$ , or IL-12 and IL-15 (R & D systems).

In figure 7, splenocytes were incubated with or without 50 $\mu$ g/mL  $\alpha$ IL-12 (C17.8),  $\alpha$ IFN- $\gamma$  (XM1.2),  $\alpha$ TNF- $\alpha$  (XT22) (all produced in the Harty laboratory at the University of Iowa), or a mix of all anti-cytokines in the presence of 200nM NP<sub>396</sub> peptide.

Following incubation, surface staining was conducted by incubating splenocytes with antibody cocktails for 20 minutes at 4° C. Endogenous (Thy1.1 neg) and P14 or OT-I (Thy1.1 pos) memory cells were distinguished from one another based upon surface staining with anti-CD8 (clone 53-6.7, eBioscience) and anti-Thy1.1 (clone His51, eBioscience). In figure 3, endogenous Ag-experienced CD8 T cells and P14 cells were detected based upon surface staining with anti-



Thy1.1 (clone His51, eBioscience), anti-CD8 (clone 53-6.7, eBioscience) and anti-CD11a (clone M17/4, eBioscience) as previously described (49). Cells were then permeabilized and stained intracellularly using anti-IFN- $\gamma$  (clone XMG1.2, eBioscience). Flow cytometry data was acquired using FACSCanto (BD Biosciences, San Jose, CA) and analyzed using FloJo software (Tree Star Inc., Ashland, OR).

#### **ICS for mouse samples following stimulation with in vitro peptide-pulsed or whole pathogens**

Splenocytes from a naïve C57BL/6 mouse were collected and processed into a single-cell suspension. Cells were CFSE labeled by washing three times in PBS, incubating  $10^7$  cells/mL in room temperature PBS for 15 minutes in the presence of 5mM CFSE, incubating on ice for 5 minutes with 1mL of fetal calf serum (FCS), and washing three times with RPMI containing 10% FCS. Cells were re-suspended in RPMI containing 10% FCS.

Cells were then plated at  $5 \times 10^6$  cells per well, and RPMI containing 10% FCS, 200nM concentrations of GP<sub>33</sub> or NP<sub>396</sub> peptide, or  $5 \times 10^6$  plaque forming units (PFUs) of VacV-GP<sub>33</sub>, VacV-OVA, or VacV-NP were added to wells, and plates were incubated for 18 hours at 37° C. Following incubation, cells were washed twice with RPMI containing 10% FCS and re-suspended at  $5 \times 10^6$  cells per mL in RPMI containing 10% FCS.

$5 \times 10^4$ ,  $2.5 \times 10^5$ ,  $5 \times 10^5$ , or  $2.5 \times 10^6$  cells were plated with  $2 \times 10^6$  splenocytes from an LCMV immune mouse, or from an LCMV immune mouse that received adoptive transfer of P14 cells prior to infection. Cells were incubated for a total of 8 hours with BFA present during the entire incubation (0+8), for the final six hours of incubation (2+6), for the final four hours of incubation (4+4), or for the final hour of incubation (7+1).

598

599 Following incubation, cells were surface stained with anti-Thy1.1 (clone His51, eBioscience),  
600 anti-CD8 (clone 53-6.7, eBioscience) and anti-CD11a (clone M17/4, eBioscience). Cells were  
601 then permeabilized and stained intracellularly using anti-IFN- $\gamma$  (clone XMG1.2, eBioscience).  
602 data was acquired using FACSCanto (BD Biosciences, San Jose, CA) and analyzed using  
603 FloJo software (Tree Star Inc., Ashland, OR).

604

605 In supplemental figure 5, splenocytes from an LCMV immune mouse containing P14 cells were  
606 mixed with CFSE- labeled splenocytes from an LM-OVA/B8R immune mouse.  $4 \times 10^6$  cells  
607 were then plated and incubated for 12, 16, or 20 hours with  $5 \times 10^6$  PFUs of VacV-GP<sub>33</sub> or  $1 \times 10^7$   
608 CFUs of LM-OVA/B8R and with or without  $50 \mu\text{g/mL}$   $\alpha\text{IL-12}$ ,  $\alpha\text{IFN-}\gamma$ ,  $\alpha\text{TNF-}\alpha$ , or a mix of all  
609 anti-cytokines, and with BFA present for the final four hours of incubation.

610

#### 611 **Quantitative RT-PCR**

612 Spleens of mice containing memory P14 cells were collected and tissue was processed into  
613 single-cell suspension. Cells were plated and incubated with  $200 \text{ nM}$  NP<sub>396</sub> peptide for a total of  
614 8 hours with BFA present for the entire incubation (0+8) or for the final hour of incubation (7+1).  
615 Cells were then surface stained for CD8 and Thy1.1 and purified with anti-PE magnetic bead  
616 sorting (Miltenyi Biotec) using standard protocols. P14 cells were then sorted from purified cells  
617 using a BD FACS Aria II (BD Biosciences). Total RNA was reverse-transcribed using a  
618 QuantiTech Reverse Transcription Kit (Qiagen), and cDNA was analyzed for expression of  
619 *Il12rb2*, *Ifngr1*, *Ifngr2*, and *Tnfrsf1b* by quantitative PCR using SYBR Advantage qPCR premix  
620 (Clontech) on an ABI 7300 Real Time PCR System (Applied Biosystems). Relative gene  
621 expression levels in each sample were normalized to that of a housekeeping gene,  
622 hypoxanthine phosphoribosyltransferase 1 (*Hprt1*).

Primers used were as follows:

*Il12rb2*: 5'- GTGTCTGCAGCCAACTCAAA and 3'- AGGCTGCCAGGTCACTAGAA

*Ifngr1*: 5'- GCTGGGTCCACTCTGCAAAT and 3'- GGCTTTGAGTAGCTTTTCAGTTCAA

*Ifngr2*: 5'- GTGCTCCAAACACCGTGAAC and 3'- GCCACGTTGCCAGTAATGAG

*Tnfrsf1b*: 5'- TTGGGGCCGACTTGTTAAGG and 3'- TGGCTGTAAAGGTGGGATGG

## Statistics

Statistical analyses were performed using GraphPad Prism software version 6 (GraphPad Software Inc.). Statistical comparisons of cytokine production by samples that were incubated in the presence of BFA for the entire incubation (0+8 or 0+20) compared to samples that were incubated with BFA for the final hour (7+1) or final four hours (16+4), or for mRNA expression of cytokine receptors for cells that were incubated in the presence of BFA for the entire incubation (0+8) compared to samples that were incubated with BFA for the final hour (7+1) were done using the paired 2-tailed student *t*-test, and a *p* value of less than 0.05 was considered significant. Statistical comparisons of cytokine production by human samples that were incubated in the presence of peptide pools and in the presence or absence of anti-cytokines and with BFA present for the entire incubation or the final four hours of incubation were done using a non-parametric ANOVA with repeated measures (Freedman's Test) with Dunn's post-hoc test for multiple comparisons with respect to 0+20 samples, and a *p* value of less than 0.05 was considered significant.

## Study Approval

Human studies involving malaria vaccinated subjects were approved by the NIAID Institutional Review Board as described (63). All patients gave written informed consent. For blood donations collected from human patients at the University of Iowa, PBMCs were obtained from anonymous donors at the DeGowin Blood Center at the University of Iowa, and no identifying

information was collected from donors. Donors consented to allow blood cells not used for donation to be used for purposes of research. The consent process and documents for these donors have been approved by the IRB for the University of Iowa. All experiments involving animals were approved by the IACUC of the University of Iowa.

#### **Author Contributions**

M.D.M., I.J.J., A.S.I., Q.S., H.H.X., R.A.S., J.T.H., and V.P.B. designed the research studies; M.D.M., I.J.J., M.L., Q.S., and A.S.I. performed the research and analyzed the data; M.D.M., I.J.J., A.S.I., Q.S., R.A.S., J.T.H., and V.P.B. discussed the results and implications; and M.D.M., A.S.I., J.T.H., R.A.S., and V.P.B. wrote the paper.

#### **Acknowledgements**

The authors wish to thank Christina Winborn for help with maintenance of mouse colonies, and Christina Winborn, Stacey Hartwig, and Lecia Epping for preparation of reagents used in this study. Human sample analyses were supported by the Intramural Research Program of the US National Institutes of Health. Some of the data presented herein were obtained at the Flow Cytometry Facility, which is a Carver College of Medicine/ Holden Comprehensive Cancer Center core research facility at the University of Iowa. The facility is funded through user fees and the generous financial support of the Carver College of Medicine, Holden Comprehensive Cancer Center, and Iowa City Veteran's Administration Medical Center. Research utilizing the FACSria was supported by the National Center for Research Resources of the National Institutes of Health under Award Number 1 S10OD016199-01A1. This work was supported by NIH grants AI42767, AI85515, and AI100527 (JTH), AI114543 (JTH and VPB), GM113961 (VPB), AI139874 (HHX), and T32AI007485 and T32AI007511 (IJJ), by Veteran Affairs BLR&D Merit Review Program BX002903A (HHX), and by NCI award 4T32AI007260-30 (The Holden Comprehensive Cancer Center).

## References

1. Masopust D. Developing an HIV cytotoxic T-lymphocyte vaccine: issues of CD8 T-cell quantity, quality and location. *J Intern Med*. 2009;265(1):125-37.
2. Brown LE, and Kelso A. Prospects for an influenza vaccine that induces cross-protective cytotoxic T lymphocytes. *Immunol Cell Biol*. 2009;87(4):300-8.
3. Thomas PG, Keating R, Hulse-Post DJ, and Doherty PC. Cell-mediated protection in influenza infection. *Emerg Infect Dis*. 2006;12(1):48-54.
4. Epstein JE, Tewari K, Lyke KE, Sim BK, Billingsley PF, Laurens MB, et al. Live attenuated malaria vaccine designed to protect through hepatic CD8(+) T cell immunity. *Science*. 2011;334(6055):475-80.
5. Sahin U, Derhovanessian E, Miller M, Kloke BP, Simon P, Lower M, et al. Personalized RNA mutanome vaccines mobilize poly-specific therapeutic immunity against cancer. *Nature*. 2017;547(7662):222-6.
6. Seder RA, Chang LJ, Enama ME, Zephir KL, Sarwar UN, Gordon IJ, et al. Protection against malaria by intravenous immunization with a nonreplicating sporozoite vaccine. *Science*. 2013;341(6152):1359-65.
7. Schmidt NW, Podyminogin RL, Butler NS, Badovinac VP, Tucker BJ, Bahjat KS, et al. Memory CD8 T cell responses exceeding a large but definable threshold provide long-term immunity to malaria. *Proc Natl Acad Sci U S A*. 2008;105(37):14017-22.
8. Wolfl M, Kuball J, Ho WY, Nguyen H, Manley TJ, Bleakley M, et al. Activation-induced expression of CD137 permits detection, isolation, and expansion of the full repertoire of CD8+ T cells responding to antigen without requiring knowledge of epitope specificities. *Blood*. 2007;110(1):201-10.
9. Bansal A, Mann T, Sterrett S, Peng BJ, Bet A, Carlson JM, et al. Enhanced Recognition of HIV-1 Cryptic Epitopes Restricted by HLA Class I Alleles Associated With a Favorable Clinical Outcome. *J Acquir Immune Defic Syndr*. 2015;70(1):1-8.
10. Chu H, George SL, Stinchcomb DT, Osorio JE, and Partidos CD. CD8+ T-cell Responses in Flavivirus-Naive Individuals Following Immunization with a Live-Attenuated Tetravalent Dengue Vaccine Candidate. *J Infect Dis*. 2015;212(10):1618-28.
11. Smith KN, Mailliard RB, Larsen BB, Wong K, Gupta P, Mullins JI, et al. Dendritic cells restore CD8+ T cell reactivity to autologous HIV-1. *J Virol*. 2014;88(17):9976-90.
12. Turtle L, Bali T, Buxton G, Chib S, Chan S, Soni M, et al. Human T cell responses to Japanese encephalitis virus in health and disease. *J Exp Med*. 2016;213(7):1331-52.
13. Kutscher S, Dembek CJ, Deckert S, Russo C, Korber N, Bogner JR, et al. Overnight resting of PBMC changes functional signatures of antigen specific T- cell responses: impact for immune monitoring within clinical trials. *PLoS One*. 2013;8(10):e76215.
14. Gold MC, Eid T, Smyk-Pearson S, Eberling Y, Swarbrick GM, Langley SM, et al. Human thymic MR1-restricted MAIT cells are innate pathogen-reactive effectors that adapt following thymic egress. *Mucosal Immunol*. 2013;6(1):35-44.
15. Fuchs YF, Jainta GW, Kuhn D, Wilhelm C, Weigelt M, Karasinsky A, et al. Vagaries of the ELISpot assay: specific detection of antigen responsive cells requires purified CD8(+) T

- cells and MHC class I expressing antigen presenting cell lines. *Clin Immunol.* 2015;157(2):216-25.
16. Wipasa J, Wongkulab P, Chawansuntati K, Chaiwarit R, and Supparatpinyo K. Cellular immune responses in HIV-negative immunodeficiency with anti-interferon-gamma antibodies and opportunistic intracellular microorganisms. *PLoS One.* 2014;9(10):e110276.
  17. Kelly C, Swadling L, Capone S, Brown A, Richardson R, Halliday J, et al. Chronic hepatitis C viral infection subverts vaccine-induced T-cell immunity in humans. *Hepatology.* 2016;63(5):1455-70.
  18. Riddell NE, Griffiths SJ, Rivino L, King DC, Teo GH, Henson SM, et al. Multifunctional cytomegalovirus (CMV)-specific CD8(+) T cells are not restricted by telomere-related senescence in young or old adults. *Immunology.* 2015;144(4):549-60.
  19. Bourguignon P, Clement F, Renaud F, Le Bras V, Koutsoukos M, Burny W, et al. Processing of blood samples influences PBMC viability and outcome of cell-mediated immune responses in antiretroviral therapy-naive HIV-1-infected patients. *J Immunol Methods.* 2014;414:1-10.
  20. Kloverpris HN, Payne RP, Sacha JB, Rasaiyaah JT, Chen F, Takiguchi M, et al. Early antigen presentation of protective HIV-1 KF11Gag and KK10Gag epitopes from incoming viral particles facilitates rapid recognition of infected cells by specific CD8+ T cells. *J Virol.* 2013;87(5):2628-38.
  21. Bacher P, Schink C, Teutschbein J, Kniemeyer O, Assenmacher M, Brakhage AA, et al. Antigen-reactive T cell enrichment for direct, high-resolution analysis of the human naive and memory Th cell repertoire. *J Immunol.* 2013;190(8):3967-76.
  22. Kagina BM, Mansoor N, Kpamegan EP, Penn-Nicholson A, Nemes E, Smit E, et al. Qualification of a whole blood intracellular cytokine staining assay to measure mycobacteria-specific CD4 and CD8 T cell immunity by flow cytometry. *J Immunol Methods.* 2015;417:22-33.
  23. Singh SK, Meyering M, Ramwadhoebe TH, Stynebosch LF, Redeker A, Kuppen PJ, et al. The simultaneous ex vivo detection of low-frequency antigen-specific CD4+ and CD8+ T-cell responses using overlapping peptide pools. *Cancer Immunol Immunother.* 2012;61(11):1953-63.
  24. Mingozzi F, Meulenberg JJ, Hui DJ, Basner-Tschakarjan E, Hasbrouck NC, Edmonson SA, et al. AAV-1-mediated gene transfer to skeletal muscle in humans results in dose-dependent activation of capsid-specific T cells. *Blood.* 2009;114(10):2077-86.
  25. Rezvani K, Yong AS, Mielke S, Savani BN, Musse L, Superata J, et al. Leukemia-associated antigen-specific T-cell responses following combined PR1 and WT1 peptide vaccination in patients with myeloid malignancies. *Blood.* 2008;111(1):236-42.
  26. Guihot A, Oksenhendler E, Galicier L, Marcelin AG, Papagno L, Bedin AS, et al. Multicentric Castleman disease is associated with polyfunctional effector memory HHV-8-specific CD8+ T cells. *Blood.* 2008;111(3):1387-95.
  27. Rezvani K, Yong AS, Savani BN, Mielke S, Keyvanfar K, Gostick E, et al. Graft-versus-leukemia effects associated with detectable Wilms tumor-1 specific T lymphocytes after allogeneic stem-cell transplantation for acute lymphoblastic leukemia. *Blood.* 2007;110(6):1924-32.

- 762 28. Tae Yu H, Youn JC, Lee J, Park S, Chi HS, Lee J, et al. Characterization of CD8(+)CD57(+) T  
763 cells in patients with acute myocardial infarction. *Cell Mol Immunol*. 2015;12(4):466-73.
- 764 29. Spielmann G, Bollard CM, Kunz H, Hanley PJ, and Simpson RJ. A single exercise bout  
765 enhances the manufacture of viral-specific T-cells from healthy donors: implications for  
766 allogeneic adoptive transfer immunotherapy. *Sci Rep*. 2016;6:25852.
- 767 30. Pulko V, Davies JS, Martinez C, Lanteri MC, Busch MP, Diamond MS, et al. Human  
768 memory T cells with a naive phenotype accumulate with aging and respond to  
769 persistent viruses. *Nat Immunol*. 2016;17(8):966-75.
- 770 31. Rivino L, Kumaran EA, Thein TL, Too CT, Gan VC, Hanson BJ, et al. Virus-specific T  
771 lymphocytes home to the skin during natural dengue infection. *Sci Transl Med*.  
772 2015;7(278):278ra35.
- 773 32. Smaill F, Jeyanathan M, Smieja M, Medina MF, Thantrige-Don N, Zganiacz A, et al. A  
774 human type 5 adenovirus-based tuberculosis vaccine induces robust T cell responses in  
775 humans despite preexisting anti-adenovirus immunity. *Sci Transl Med*.  
776 2013;5(205):205ra134.
- 777 33. Swadling L, Capone S, Antrobus RD, Brown A, Richardson R, Newell EW, et al. A human  
778 vaccine strategy based on chimpanzee adenoviral and MVA vectors that primes, boosts,  
779 and sustains functional HCV-specific T cell memory. *Sci Transl Med*.  
780 2014;6(261):261ra153.
- 781 34. Maldonado L, Teague JE, Morrow MP, Jotova I, Wu TC, Wang C, et al. Intramuscular  
782 therapeutic vaccination targeting HPV16 induces T cell responses that localize in  
783 mucosal lesions. *Sci Transl Med*. 2014;6(221):221ra13.
- 784 35. Green CA, Scarselli E, Sande CJ, Thompson AJ, de Lara CM, Taylor KS, et al. Chimpanzee  
785 adenovirus- and MVA-vectored respiratory syncytial virus vaccine is safe and  
786 immunogenic in adults. *Sci Transl Med*. 2015;7(300):300ra126.
- 787 36. Ogwang C, Kimani D, Edwards NJ, Roberts R, Mwacharo J, Bowyer G, et al. Prime-boost  
788 vaccination with chimpanzee adenovirus and modified vaccinia Ankara encoding TRAP  
789 provides partial protection against Plasmodium falciparum infection in Kenyan adults.  
790 *Sci Transl Med*. 2015;7(286):286re5.
- 791 37. Ewer KJ, O'Hara GA, Duncan CJ, Collins KA, Sheehy SH, Reyes-Sandoval A, et al.  
792 Protective CD8+ T-cell immunity to human malaria induced by chimpanzee adenovirus-  
793 MVA immunisation. *Nat Commun*. 2013;4:2836.
- 794 38. Barnes E, Folgori A, Capone S, Swadling L, Aston S, Kurioka A, et al. Novel adenovirus-  
795 based vaccines induce broad and sustained T cell responses to HCV in man. *Sci Transl*  
796 *Med*. 2012;4(115):115ra1.
- 797 39. Bagarazzi ML, Yan J, Morrow MP, Shen X, Parker RL, Lee JC, et al. Immunotherapy  
798 against HPV16/18 generates potent TH1 and cytotoxic cellular immune responses. *Sci*  
799 *Transl Med*. 2012;4(155):155ra38.
- 800 40. Berg RE, Cordes CJ, and Forman J. Contribution of CD8+ T cells to innate immunity: IFN-  
801 gamma secretion induced by IL-12 and IL-18. *Eur J Immunol*. 2002;32(10):2807-16.
- 802 41. Berg RE, Crossley E, Murray S, and Forman J. Memory CD8+ T cells provide innate  
803 immune protection against *Listeria monocytogenes* in the absence of cognate antigen. *J*  
804 *Exp Med*. 2003;198(10):1583-93.

- 805 42. Freeman BE, Hammarlund E, Raue HP, and Slifka MK. Regulation of innate CD8+ T-cell  
806 activation mediated by cytokines. *Proc Natl Acad Sci U S A*. 2012;109(25):9971-6.
- 807 43. Luke TC, and Hoffman SL. Rationale and plans for developing a non-replicating,  
808 metabolically active, radiation-attenuated *Plasmodium falciparum* sporozoite vaccine. *J*  
809 *Exp Biol*. 2003;206(Pt 21):3803-8.
- 810 44. Brophy SE, Jones LL, Holler PD, and Kranz DM. Cellular uptake followed by class I MHC  
811 presentation of some exogenous peptides contributes to T cell stimulatory capacity. *Mol*  
812 *Immunol*. 2007;44(9):2184-94.
- 813 45. Homann D, Teyton L, and Oldstone MB. Differential regulation of antiviral T-cell  
814 immunity results in stable CD8+ but declining CD4+ T-cell memory. *Nat Med*.  
815 2001;7(8):913-9.
- 816 46. Martin MD, Shan Q, Xue HH, and Badovinac VP. Time and Antigen-Stimulation History  
817 Influence Memory CD8 T Cell Bystander Responses. *Front Immunol*. 2017;8:634.
- 818 47. Thome JJ, Yudanin N, Ohmura Y, Kubota M, Grinshpun B, Sathaliyawala T, et al. Spatial  
819 map of human T cell compartmentalization and maintenance over decades of life. *Cell*.  
820 2014;159(4):814-28.
- 821 48. Odumade OA, Knight JA, Schmeling DO, Masopust D, Balfour HH, Jr., and Hogquist KA.  
822 Primary Epstein-Barr virus infection does not erode preexisting CD8(+) T cell memory in  
823 humans. *J Exp Med*. 2012;209(3):471-8.
- 824 49. Rai D, Pham NL, Harty JT, and Badovinac VP. Tracking the total CD8 T cell response to  
825 infection reveals substantial discordance in magnitude and kinetics between inbred and  
826 outbred hosts. *J Immunol*. 2009;183(12):7672-81.
- 827 50. Martin MD, Danahy DB, Hartwig SM, Harty JT, and Badovinac VP. Revealing the  
828 Complexity in CD8 T Cell Responses to Infection in Inbred C57B/6 versus Outbred Swiss  
829 Mice. *Front Immunol*. 2017;8:1527.
- 830 51. Papadakis KA, Prehn JL, Landers C, Han Q, Luo X, Cha SC, et al. TL1A synergizes with IL-12  
831 and IL-18 to enhance IFN-gamma production in human T cells and NK cells. *J Immunol*.  
832 2004;172(11):7002-7.
- 833 52. Smeltz RB. Profound enhancement of the IL-12/IL-18 pathway of IFN-gamma secretion  
834 in human CD8+ memory T cell subsets via IL-15. *J Immunol*. 2007;178(8):4786-92.
- 835 53. Bou Ghanem EN, and D'Orazio SE. Human CD8+ T cells display a differential ability to  
836 undergo cytokine-driven bystander activation. *Cell Immunol*. 2011;272(1):79-86.
- 837 54. Letimier FA, Passini N, Gasparian S, Bianchi E, and Rogge L. Chromatin remodeling by the  
838 SWI/SNF-like BAF complex and STAT4 activation synergistically induce IL-12Rbeta2  
839 expression during human Th1 cell differentiation. *EMBO J*. 2007;26(5):1292-302.
- 840 55. Li J, Yin Q, and Wu H. Structural basis of signal transduction in the TNF receptor  
841 superfamily. *Adv Immunol*. 2013;119:135-53.
- 842 56. Plataniias LC. Mechanisms of type-I- and type-II-interferon-mediated signalling. *Nat Rev*  
843 *Immunol*. 2005;5(5):375-86.
- 844 57. Bijker EM, Teirlinck AC, Schats R, van Gemert GJ, van de Vegte-Bolmer M, van Lieshout  
845 L, et al. Cytotoxic markers associate with protection against malaria in human  
846 volunteers immunized with *Plasmodium falciparum* sporozoites. *J Infect Dis*.  
847 2014;210(10):1605-15.



58. Bastiaens GJ, van Meer MP, Scholzen A, Obiero JM, Vatanashenassan M, van Grinsven T, et al. Safety, Immunogenicity, and Protective Efficacy of Intradermal Immunization with Aseptic, Purified, Cryopreserved Plasmodium falciparum Sporozoites in Volunteers Under Chloroquine Prophylaxis: A Randomized Controlled Trial. *Am J Trop Med Hyg.* 2016;94(3):663-73.
59. Van Braeckel-Budimir N, Gras S, Ladell K, Josephs TM, Pewe L, Urban SL, et al. A T Cell Receptor Locus Harbors a Malaria-Specific Immune Response Gene. *Immunity.* 2017;47(5):835-47 e4.
60. Navarrete MA. ELISpot and DC-ELISpot Assay to Measure Frequency of Antigen-Specific IFN $\gamma$ -Secreting Cells. *Methods Mol Biol.* 2015;1318:79-86.
61. Altman JD, Moss PA, Goulder PJ, Barouch DH, McHeyzer-Williams MG, Bell JL, et al. Phenotypic analysis of antigen-specific T lymphocytes. *Science.* 1996;274(5284):94-6.
62. Nolz JC, Rai D, Badovinac VP, and Harty JT. Division-linked generation of death-intermediates regulates the numerical stability of memory CD8 T cells. *Proc Natl Acad Sci U S A.* 2012;109(16):6199-204.
63. Ishizuka AS, Lyke KE, DeZure A, Berry AA, Richie TL, Mendoza FH, et al. Protection against malaria at 1 year and immune correlates following PfSPZ vaccination. *Nat Med.* 2016;22(6):614-23.
64. Hoffman SL, Billingsley PF, James E, Richman A, Loyevsky M, Li T, et al. Development of a metabolically active, non-replicating sporozoite vaccine to prevent Plasmodium falciparum malaria. *Hum Vaccin.* 2010;6(1):97-106.
65. Lyke KE, Ishizuka AS, Berry AA, Chakravarty S, DeZure A, Enama ME, et al. Attenuated PfSPZ Vaccine induces strain-transcending T cells and durable protection against heterologous controlled human malaria infection. *Proc Natl Acad Sci U S A.* 2017;114(10):2711-6.

Figure 1

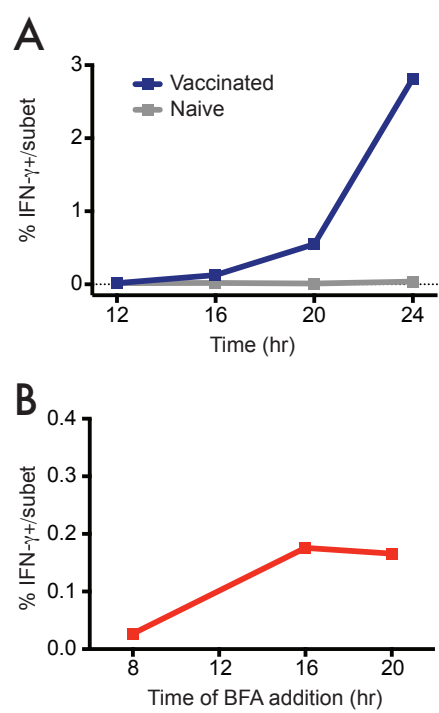
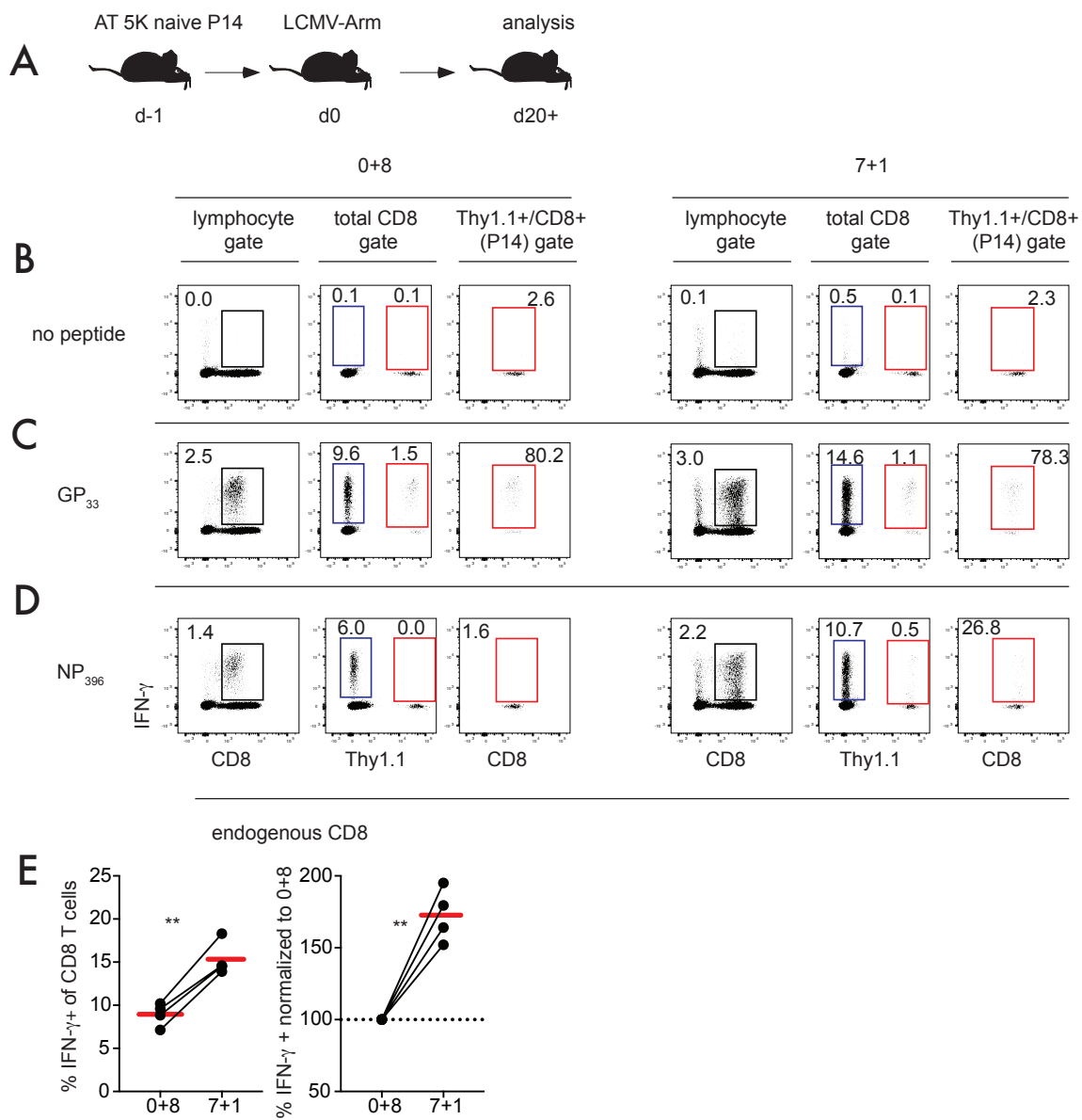


**Figure 1. Increased length of incubation and delayed addition of BFA lead to elevated detection of IFN- $\gamma$  producing human CD8 T cells following PfSPZ stimulation. (A)**

Percentage of CD8 T cells producing IFN- $\gamma$  when PBMCs from a PfSPZ vaccinated or unvaccinated (naïve) subject were stimulated with PfSPZ for 12, 16, 20, or 24 hours. **(B)**

Percentage of CD8 T cells producing IFN- $\gamma$  when PBMCs from a PfSPZ vaccinated subject were stimulated with PfSPZ for a total of 24 hours with BrefeldinA (BFA) addition occurring after the first 8, 16, or 20 hours. n=1

Figure 2

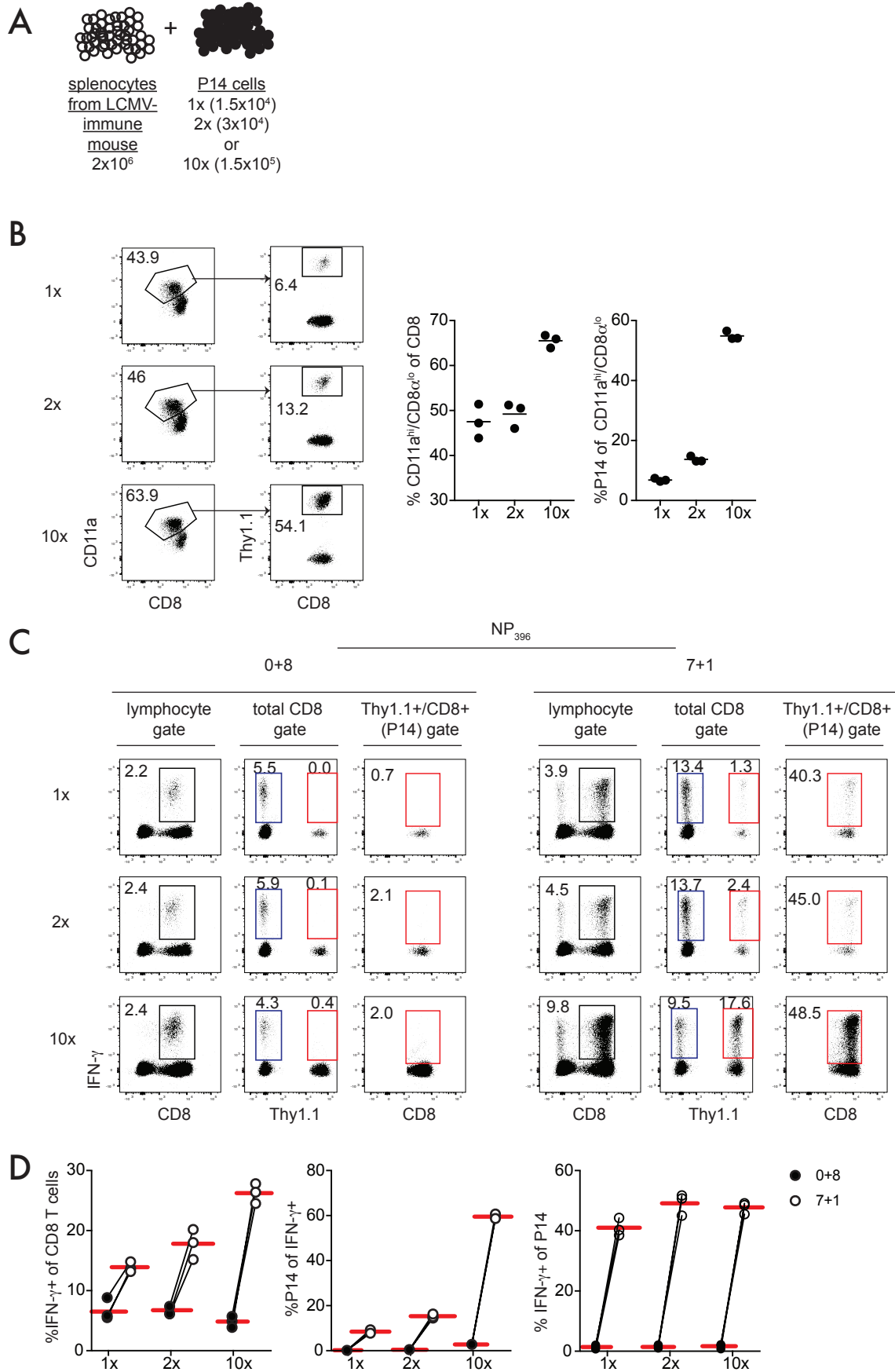


883 **Figure 2. Delayed addition of BFA leads to bystander activation of CD8 T cells. (A)**

884 Experimental design. Mice received adoptive transfer (AT) of naïve P14 cells and were infected  
 885 with LCMV-Armstrong. Approximately three weeks after infection, splenocytes were harvested  
 886 and ICS was conducted. **(B)** Representative dot plots of IFN- $\gamma$  production following 8 hour  
 887 incubation without peptide and with BFA present the entire incubation (0+8), or the final hour  
 888 (7+1). Plots on the left are gated lymphocytes, plots in the middle are gated CD8 T cells (Thy1.1  
 889 neg= endogenous CD8 T cells, and Thy1.1 pos= P14 cells), and plots on the right are gated  
 890 P14 cells. Numbers inside plots indicate the percentage of cells producing IFN- $\gamma$  out of all gated  
 891 cells. **(C)** Representative dot plots of IFN- $\gamma$  production following 8 hour incubation with GP<sub>33</sub>  
 892 peptide. **(D)** Representative dot plots of IFN- $\gamma$  production following 8 hour incubation with NP<sub>396</sub>  
 893 peptide. **(E)** Left- summary graphs of the percentage of endogenous CD8 T cells producing  
 894 IFN- $\gamma$  following stimulation with GP<sub>33</sub> peptide out of all CD8 T cells with BFA present the entire  
 895 incubation (0+8), or the final hour (7+1). Right- percentage of endogenous CD8 T cells  
 896 producing IFN- $\gamma$  when BFA was added the final hour of incubation normalized to the percentage  
 897 when BFA was present the entire incubation (100%- dotted line). Representative data from  
 898 greater than 3 independent experiments. n=4. Dots indicate individual mice. Solid red lines  
 899 indicate the mean. \*\*p<0.01 as determined by paired student t test.

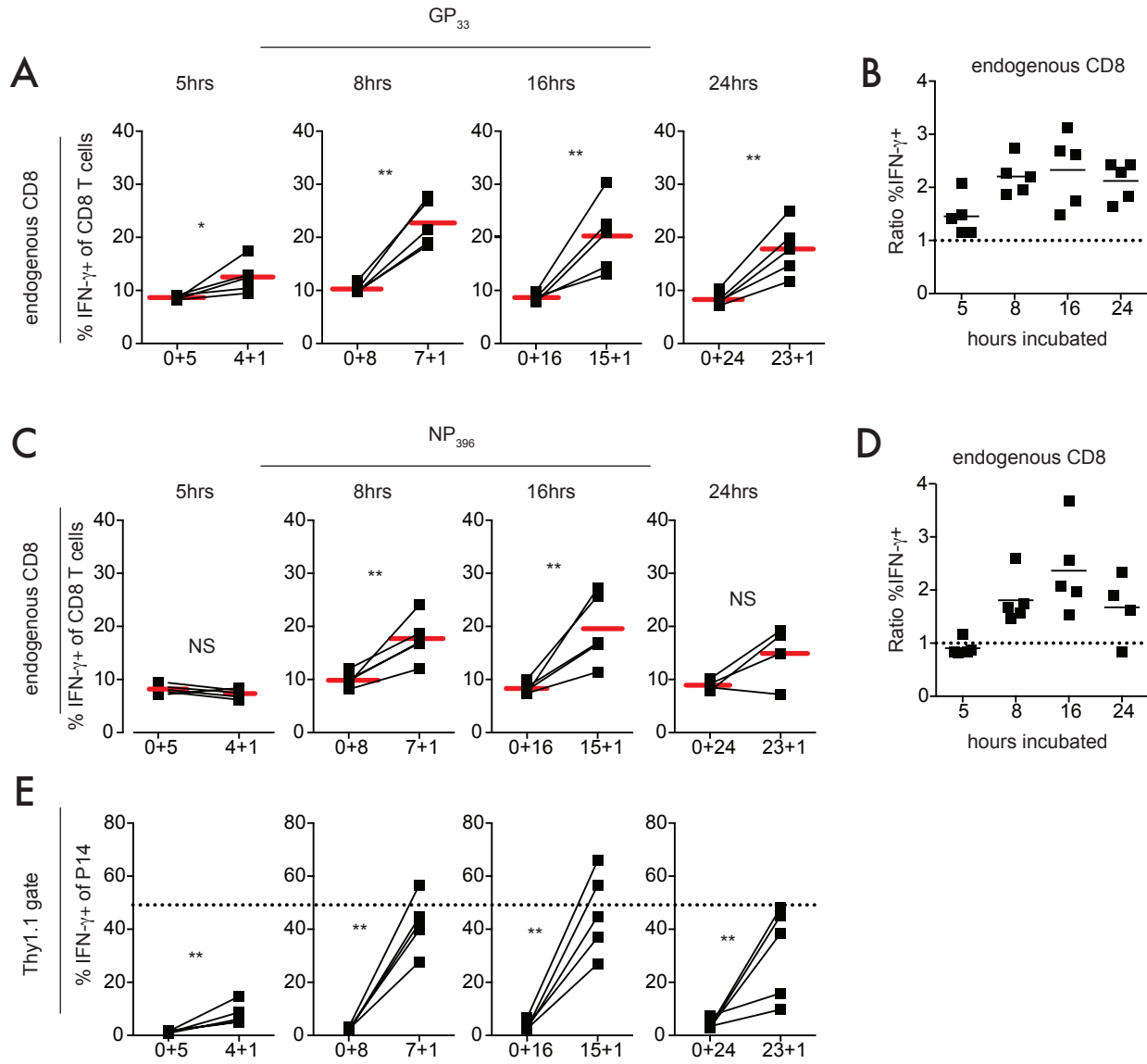
900

Figure 3



**Figure 3. Contribution of bystander responses to IFN- $\gamma$  producing cells detected when addition of BFA is delayed is influenced by CD8 T cell pool composition.** **(A)** Experimental design. Prior to 8 hour incubation with NP<sub>396</sub> peptide, splenocytes from an LCMV-Armstrong immune mouse were mixed with different numbers of sorted memory P14 cells. **(B)** Left- representative dot plots of Ag-experienced (CD11ahi/CD8lo) CD8 T cells among all CD8 T cells (left plot) and percentage of P14 cells (Thy1.1 pos) among Ag-experienced CD8 T cells (right plot) after mixing. Middle- summary graph of the percentage of Ag-experienced CD8 T cells among all CD8 T cells after mixing. Right- summary graph of the percentage of memory P14 cells among Ag-experienced CD8 T cells after mixing. **(C)** Representative dot plots of IFN- $\gamma$  production following 8 hour incubation with NP<sub>396</sub> peptide and with BFA present the entire incubation (0+8), or the final hour (7+1). Plots on the left are gated lymphocytes, plots in the middle are gated CD8 T cells (Thy1.1 neg= endogenous CD8 T cells, and Thy1.1 pos= P14 cells), and plots on the right are gated P14 cells. Numbers inside plots indicate the percentage of cells producing IFN- $\gamma$  out of all gated cells. **(D)** Left- summary graphs of the percentage of CD8 T cells producing IFN- $\gamma$  out of all CD8 T cells with BFA present the entire incubation (0+8), or the final hour (7+1). Middle- summary graphs of the percentage of P14 cells producing IFN- $\gamma$  out of all IFN- $\gamma$ + CD8 T cells with BFA present the entire incubation (0+8), or the final hour (7+1). Right- summary graphs of the percentage of gated P14 cells producing IFN- $\gamma$  with BFA present the entire incubation (0+8), or the final hour (7+1). Representative data from 2 independent experiments. n=3. Dots indicate individual mice. Solid red lines indicate the mean.

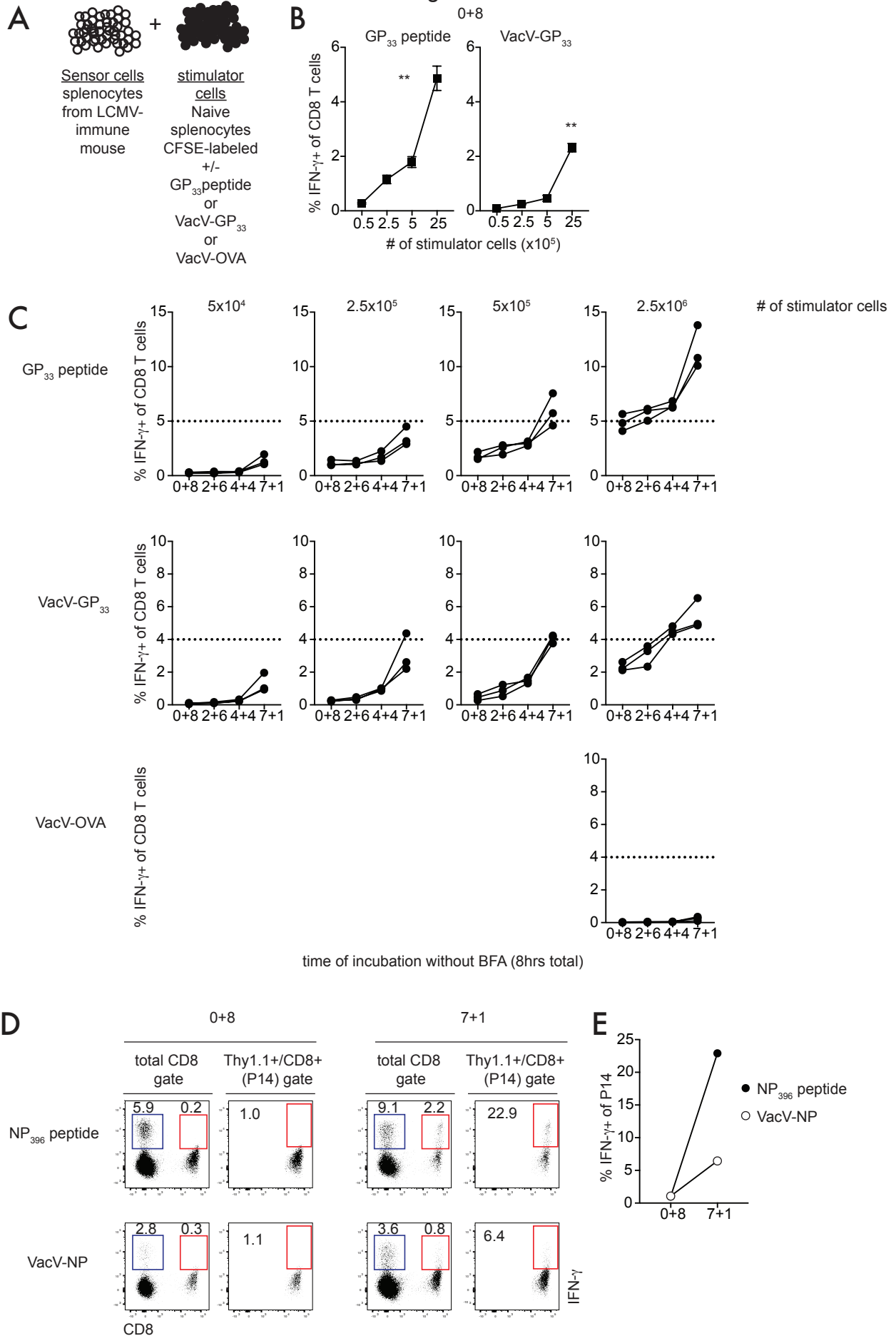
Figure 4





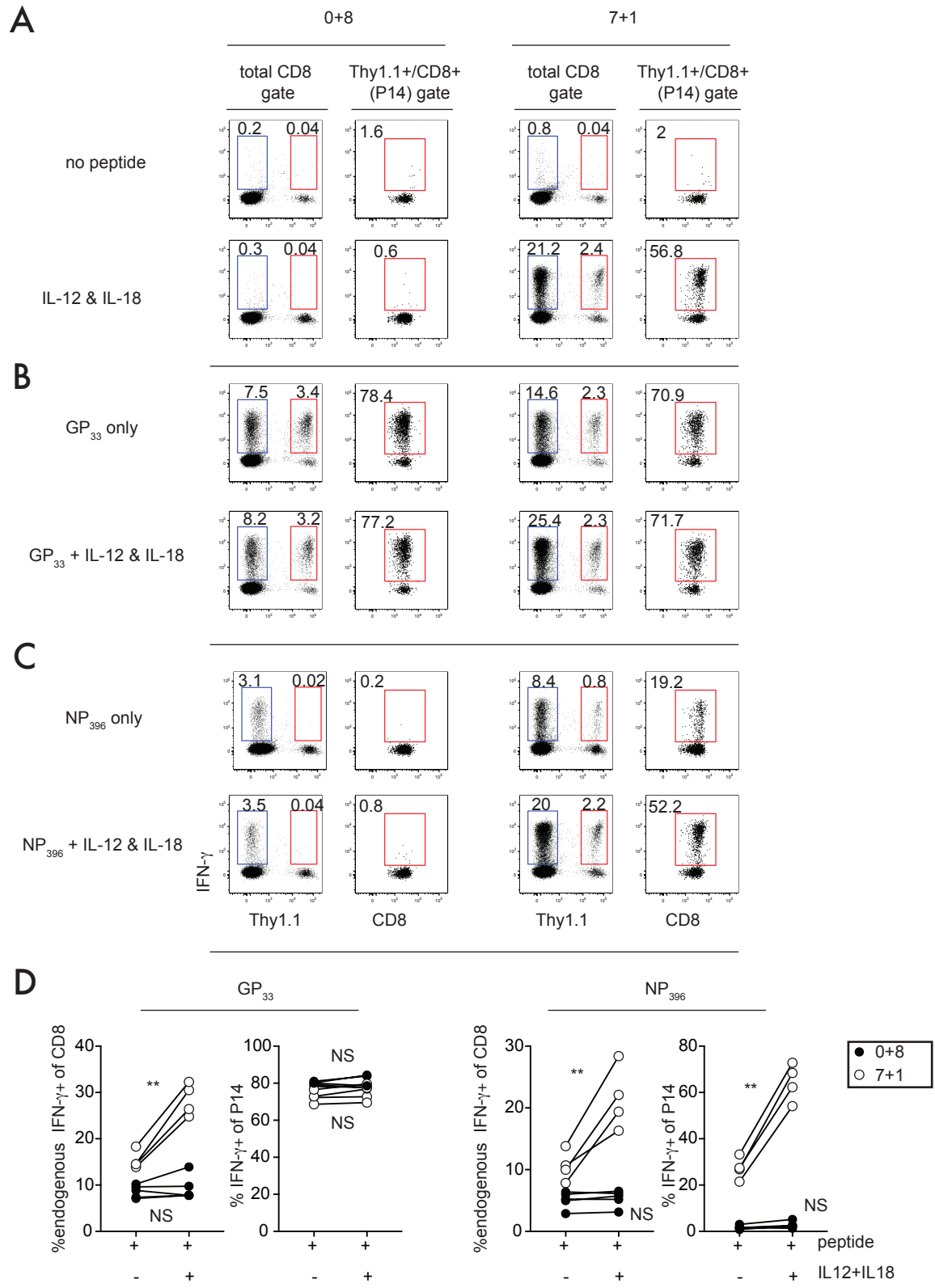
**Figure 4. Contribution of bystander responses to IFN- $\gamma$  producing cells detected when BFA addition is delayed increases with extended length of stimulation but is seen following incubation times of 5 or more hours.** Mice received adoptive transfer of naïve P14 cells and were infected with LCMV-Armstrong. ICS was conducted with GP<sub>33</sub> **(A-B)** or NP<sub>396</sub> **(C-D)** peptide approximately three weeks after infection. Total incubation times were 5, 8, 16, or 24 hours with BFA present the whole incubation or the final hour. **(A)** Summary graphs of the percentage of endogenous (Thy1.1 neg) CD8 T cells producing IFN- $\gamma$  out of all endogenous CD8 T cells with BFA present the entire incubation, or the final hour. **(B)** Ratio of the percentage of endogenous CD8 T cells producing IFN- $\gamma$  when BFA was present the final hour of incubation over the percentage of endogenous CD8 T cells producing IFN- $\gamma$  when BFA was present the entire incubation. **(C)** Top- summary graphs of the percentage of endogenous (Thy1.1 neg) CD8 T cells producing IFN- $\gamma$  out of all endogenous CD8 T cells with BFA present the entire incubation, or the final hour. Bottom- summary graphs of the percentage of P14 cells (Thy1.1 pos) producing IFN- $\gamma$  out of all P14 cells with BFA present the entire incubation, or the final hour. **(D)** Ratio of the percentage of endogenous CD8 T cells producing IFN- $\gamma$  when BFA was present the final hour of incubation over the percentage of endogenous CD8 T cells producing IFN- $\gamma$  when BFA was present the entire incubation. Representative data from greater than 3 independent experiments. n=5. Dots indicate individual mice. Solid lines indicate the mean. NS=not significant, \*p<0.05, \*\*p<0.01 as determined by paired student t test.

Figure 5



**Figure 5. Delayed BFA addition leads to bystander activation of CD8 T cells following stimulation with pathogen-infected splenocytes. (A)** Experimental design. Splenocytes from a naïve mouse (stimulator cells) were CFSE-labeled and either pulsed with GP<sub>33</sub> peptide or infected with VacV–GP<sub>33</sub> or VacV–OVA. Stimulator cells were mixed with splenocytes from an LCMV–Armstrong immune mouse (sensor cells) and incubated for 8 hours with BFA present for 8 (0+8), 6 (2+6), 4 (4+4), or 1 (7+1) hours. **(B)** CD8 T cells producing IFN- $\gamma$  after 8 hour incubation with indicated numbers of GP<sub>33</sub> peptide pulsed (left), or VacV–GP<sub>33</sub> infected (right) stimulator cells with BFA present the entire incubation. **(C)** Top- CD8 T cells producing IFN- $\gamma$  after incubation with indicated numbers of GP<sub>33</sub> peptide- pulsed stimulator cells and with BFA the indicated times. Middle- CD8 T cells producing IFN- $\gamma$  after incubation with indicated numbers of VacV–GP<sub>33</sub> infected stimulator cells and with BFA the indicated times. Bottom- CD8 T cells producing IFN- $\gamma$  after incubation with indicated numbers of VacV–OVA infected stimulator cells and with BFA the indicated times. **(D)** NP<sub>396</sub> peptide-pulsed or VacV–NP infected stimulator cells were mixed with sensor cells from an LCMV–Armstrong immune mouse containing P14 cells. Representative dot plots of IFN- $\gamma$  production by gated CD8 T cells (left plots- Thy1.1 neg= endogenous CD8 T cells, and Thy1.1 pos= P14 cells) or P14 cells (right plots). Numbers inside plots indicate the percentage of cells producing IFN- $\gamma$  out of all gated cells. **(E)** Summary graphs of the percentage of P14 cells producing IFN- $\gamma$  after stimulation with NP<sub>396</sub> pulsed (black circles) or VacV–NP infected stimulator cells (white circles) with BFA present the entire incubation (0+8) or the final hour (7+1). Representative data from 3 independent experiments. n=3. Dots indicate individual mice. \*\*p<0.01 as determined by paired student t test.

Figure 6



**Figure 6. Inflammatory cytokines trigger bystander IFN- $\gamma$  production by CD8 T cells when addition of BFA is delayed.** Mice received adoptive transfer of naïve P14 cells and were infected with LCMV-Armstrong. ICS was conducted approximately three weeks after infection.

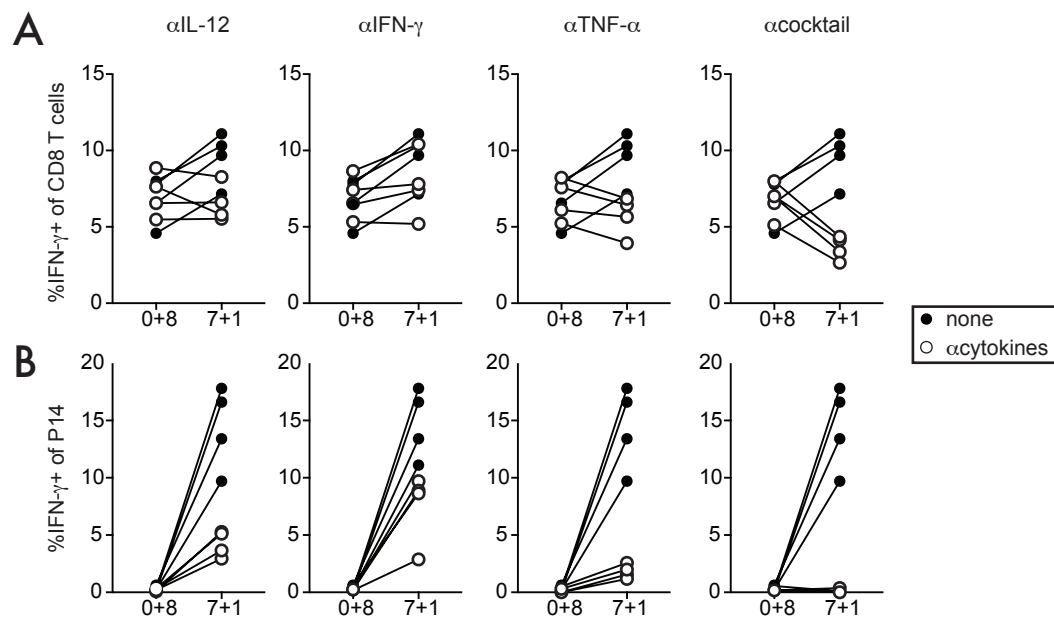
**(A)** Representative dot plots of IFN- $\gamma$  production following 8 hour incubation without peptide (top panels) or with IL-12 and IL-18 (bottom panels) and with BFA present the entire incubation (0+8), or the final hour (7+1). Plots on the left are gated CD8 T cells (Thy1.1 neg= endogenous CD8 T cells, and Thy1.1 pos= P14 cells), and plots on the right are gated P14 cells. Numbers inside plots indicate the percentage of gated cells producing IFN- $\gamma$ .

**(B)** Representative dot plots of IFN- $\gamma$  production following 8 hour incubation with GP<sub>33</sub> peptide (top panels) or with GP<sub>33</sub> peptide and IL-12 and IL-18 (bottom panels).

**(C)** Representative dot plots of IFN- $\gamma$  production following 8 hour incubation with NP<sub>396</sub> peptide (top panels) or with NP<sub>396</sub> peptide and IL-12 and IL-18 (bottom panels).

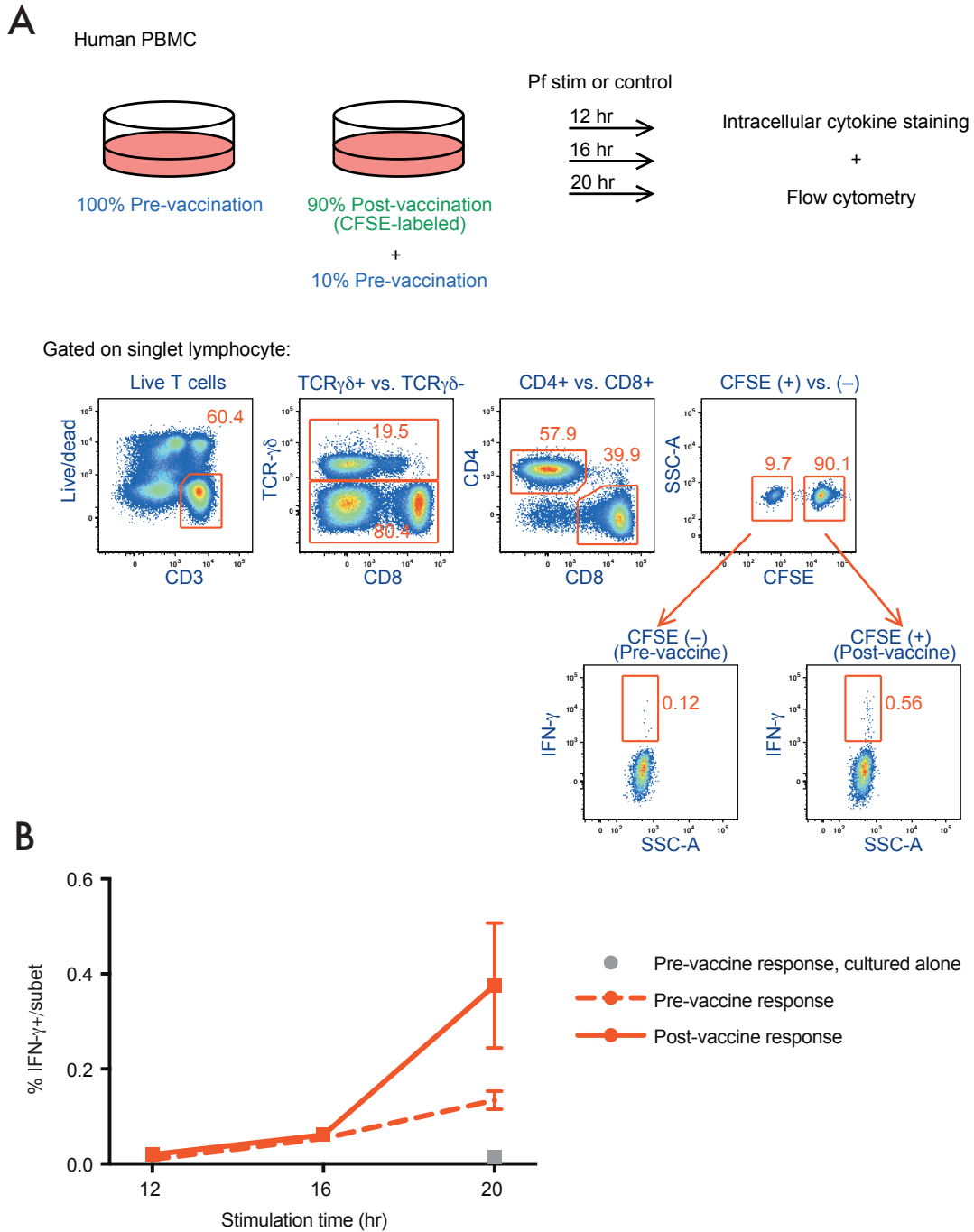
**(D)** Left- summary graphs of the percentage of endogenous CD8 T cells (left panel) and P14 cells (right panel) producing IFN- $\gamma$  after incubation with GP<sub>33</sub> peptide alone or with GP<sub>33</sub> peptide and IL-12 and IL-18 with BFA present the entire incubation (black circles) or the final hour (white circles). Right- summary graphs of the percentage of endogenous CD8 T cells (left panel) and P14 cells (right panel) producing IFN- $\gamma$  after incubation with NP<sub>396</sub> peptide alone or with NP<sub>396</sub> peptide and IL-12 and IL-18 with BFA present the entire incubation (black circles) or the final hour (white circles). Representative data from 2 independent experiments. n=4. Dots indicate individual mice. NS= not significant, \*\*p<0.01 as determined by paired student t test.

Figure 7



**Figure 7. Blocking inflammatory cytokines reduces detection of bystander activated cells when addition of BFA is delayed.** Mice received adoptive transfer of naïve P14 cells and were infected with LCMV-Armstrong. ICS was conducted approximately three weeks after infection. **(A)** Summary graphs of the percentage of endogenous CD8 T cells producing IFN- $\gamma$  after incubation with NP<sub>396</sub> peptide (black circles) or with NP<sub>396</sub> peptide and 50 $\mu$ g  $\alpha$ IL12,  $\alpha$ IFN- $\gamma$ ,  $\alpha$ TNF- $\alpha$ , or a mix of all cytokines (white circles) with BFA present the entire incubation (0+8) or the final hour (7+1). **(B)** Summary graphs of the percentage of P14 cells producing IFN- $\gamma$  after incubation with NP<sub>396</sub> peptide (black circles) or with NP<sub>396</sub> peptide and 50 $\mu$ g  $\alpha$ IL-12,  $\alpha$ IFN- $\gamma$ ,  $\alpha$ TNF- $\alpha$ , or a mix of all cytokines (white circles) with BFA present the entire incubation (0+8) or the final hour (7+1). Representative data from 2 independent experiments. n=4.

Figure 8





**Figure 8. Delayed addition of BFA leads to bystander activation of human CD8 T cells**

**following stimulation with PfSPZ.** PBMCs from PfSPZ vaccinated subjects were CFSE-labeled and mixed with non-labeled PBMCs from the same subjects (to allow for detection of bystander responses) that were collected prior to vaccination. Samples were then stimulated with PfSPZ for 12, 16, or 20 hours, and BFA was added for the last 4 hours of the incubation. PBMCs from subjects prior to vaccination were also stimulated in the absence of post-vaccination samples as a control. **(A)** Experimental design (top) and representative dot plot of the mix of pre-immunization (CFSE-neg) and post-immunization (CFSE-pos) PBMCs (bottom) following stimulation for 20 hours with PfSPZs. **(B)** Percentage of IFN- $\gamma$  producing cells detected among pre-vaccine samples cultured alone (control), among pre-vaccine cells (bystander responses) cultured with post vaccine cells, and among post-vaccine cells cultured with pre-vaccine cells following stimulation. n=3. Data are mean +/- SEM.